Effect of Changing Temperature on the Ionic Permeation Through the Cyclic GMP-Gated Channel from Vertebrate Photoreceptors

Federico Sesti,* Mario Nizzari,* and Vincent Torre‡
*INFM, ‡Dipartimento di Fisica, Università di Genova, Genoa, Italy

ABSTRACT Native cGMP-gated channels were studied in rod outer segments of the larval tiger salamander *Ambystoma tigrinum*. The α subunit of the cGMP-gated channel from bovine rods, here referred to as the wild type (w.t.), and mutant channels were heterologously expressed in *Xenopus laevis* oocytes. These channels were studied in excised membrane patches in the inside-out configuration and were activated by the addition of 100 or 500 μM cGMP. The effect of temperature on the ionic permeation was studied. The macroscopic current flowing through the native channel at +100 mV had an activation energy of 35.8, 30, 31.8, 34.5, 41.3, and 22.4 kJ mol^{-1} in the presence of Li^+, Na^+, K^+, Rb^+, Cs^+, and NH_4^+, respectively. The macroscopic current flowing through the w.t. channel at +100 mV had an activation energy of 45.2, 38.2, 37.5, 47.3, 49.4, and 38.9 kJ mol^{-1} in the presence of Li^+, Na^+, K^+, Rb^+, Cs^+, and NH_4^+, respectively. The activation energy of the macroscopic current flowing through the native and w.t. channels did not vary significantly when the ionic concentration of the permeant ion was changed between 2.5 and 110 mM. The activation energy of the single-channel current of the w.t. channel at +100 mV was 40.4 and 33 kJ mol^{-1} for Na^+ and NH_4^+, respectively. The reversal potential of biionic solutions changed significantly with temperature. These results can be used to obtain an estimate of the enthalpic and entropic contributions to the barrier of the Gibbs free energy experienced by an ion during its permeation through the open channel. These estimates indicate that the ionic permeation and selectivity of the cGMP-gated channel are controlled both by enthalpic and entropic factors and that the selectivity of the native channel for Li^+ over Na^+ is primarily caused by entropic effects.

INTRODUCTION

The ionic selectivity of the cyclic GMP-gated channel of retinal rods has been analyzed by studying the macroscopic current (Fesenko et al., 1985; Furman and Tanaka, 1990; Luehring et al., 1990; Menini, 1990; Picco and Menini, 1993) and the current flowing through a single channel (Sesti et al., 1994). The selectivity of the native channel in retinal rods based on the reversal potential is $Li^+ > Na^+ \geqslant K^+ > Rb^+ > Cs^+$ (Menini, 1990; Furman and Tanaka, 1990; Luehring et al., 1990). Ionic selectivity is usually assumed to be caused by a different profile of the Gibbs free energy of ions along the pore. A well-known theory of ionic selectivity (Eisenman and Horn, 1983), based on the analysis of hydration energies and of electrostatic interactions, has provided a limited set of possible selectivity sequences, which coincide with those commonly found in ionic channels. According to this theory, the ionic selectivity of the native cGMP-gated channel corresponds to the sequence XI, which is usually thought to be caused by an electrostatic interaction between the permeating ion and a high-energy field within the channel.

A polypeptide of about 690 amino acids, constituting a large portion of the cyclic GMP-gated channel, has recently been purified and cloned (Kaupp et al., 1989). This polypeptide, here referred to as the w.t. channel or the α subunit, forms functional channels when expressed in *Xenopus laevis* oocytes with properties similar, but not identical to, those of the channel found in situ in vertebrate rods. The mean open time of channel openings in the native channel is very brief, i.e., less than 40 μs, so it is not possible to resolve square open events (Sesti et al., 1994; Taylor and Baylor, 1995), whereas the mean open time of the w.t. channel is in the order of 1 or 2 ms (Kaupp et al., 1989; Nizzari et al., 1993). The observed differences are likely to be caused by the existence of other subunits in the native channel (Chen et al., 1993; Körschen et al., 1995). Like the native channel, the w.t. channel is moderately selective among alkali monovalent cations, but unlike the native channel, it is more selective for Na^+ than for Li^+ (Kaupp et al., 1989). The origin of selectivity of ionic channels is usually ascribed to differences in the profile of the Gibbs free energy across the channel experienced by different ions. The Gibbs free energy is composed by an enthalpic (or energetic) and an entropic term.

The purpose of this paper is to determine the physical basis of the ionic selectivity of the cyclic GMP-gated channel and in particular to evaluate the role of enthalpic and entropic contributions in its determination. To measure or at least to estimate the enthalpic and entropic contributions to the Gibbs free energy within the pore, the effect of changing the temperature on the ionic permeation can be analyzed, as in the K^+ channel from the sarcoplasmic reticulum (Miller et al., 1988).

The paper describes two kinds of experiments. The first series of experiments studied the effect of changing the temperature on the current flowing at $\pm$100 mV for the

Received for publication 6 October 1995 and in final form 14 March 1996.
Address reprint requests to Dr. Vincent Torre, Department of Physics, University of Genoa, Via Dodecaneso 33, Genoa 16146, Italy. Tel.: 39-10-3536311; Fax: 39-10-3536311; E-mail: torre@genova.infn.it.

0006-3495/96/06/2616/24 $2.00

various ions. From these data an estimate of the activation energy for the ionic permeation through the native and w.t. cyclic GMP-gated channel was obtained for ammonium and alkali monovalent cations. At +100 mV, the sequence of activation energies was $Cs^+ > Li^+ > Rb^+ > K^+ \approx Na^+ > NH_4^+$ for the native channel and $Cs^+ > Rb^+ > Li^+ > K^+ \approx Na^+ \approx NH_4^+$ for the α subunit. As the activation energy can be taken as an estimate of the enthalpic barrier (see Appendix) in both the native and w.t. channels, the enthalpic barrier is higher for Li^+ than for Na^+. As a consequence, the selectivity of the native channel for Li^+ over Na^+ cannot be explained by simple energetic or enthalpic factors. The second series of experiments analyzed the effect of temperature on the reversal potential under biionic conditions. These experiments can provide an estimate of the entropic contribution to ionic selectivity (see Appendix and Miller et al., 1988) and suggest a significant entropic contribution to the ionic selectivity in both the native and in the w.t. channels. In particular, the selectivity of the native channel for Li^+ over Na^+ is caused by a favorable entropic contribution for Li^+.

MATERIALS AND METHODS

Dissection and recording apparatus

Recordings from native channels were obtained from rod outer segments mechanically isolated from the retina of the larval tiger salamander *Ambystoma tigrinum*. The dissection was the same as that described by Sesti et al. (1994). Recordings from the w.t., i.e., the α subunit of the cyclic GMP-activated channel, and mutant channels (E363Q, E363D, E363N, E363A, E363S and E363G) were obtained from *Xenopus laevis* oocytes injected with the mRNA encoding for the α subunit and mutant channels kindly provided by Elisabeth Eismann and Benjamin U. Kaupp. The mRNA was injected into *Xenopus laevis* oocytes (H. Kähler, Institut für Entwicklungsbiologie, Hamburg, Germany; Centre National de la Recherche Scientifique, Montpellier, France) that were treated as described by Nizzari et al. (1993). Mature *Xenopus laevis* were anesthetized with 0.2% tricaine methanesulfonate (Sigma), and ovarian lobes were removed surgically. The vitelline membrane was removed under visual control in a hyperosmotic medium. Currents activated by cyclic GMP were recorded under voltage-clamp conditions from membrane patches that were excised from rod outer segments in the inside-out configuration (Hamill et al., 1981). The recording apparatus was the same as that described by Sesti et al. (1995).

Solutions

The solution filling the patch pipette was composed of the tested monovalent cation (2.5, 5, 10, 20, 50, or 110 mM), 2 mM EDTA, and 10 mM HEPES buffered to pH 7.6 with tetramethylammonium hydroxide (TMAOH). TMAOH was used to neutralize solutions, so as to have the same buffer in experiments where Na^+ was substituted for other alkali monovalent cations or NH_4^+. Neutralizing the solution with TMAOH or NaOH did not significantly affect either the macroscopic current or the single-channel current carried by Na^+. The preparation and composition of solutions were similar to those described by Sesti et al. (1995).

The perfusing chamber had 10 pipes through which different solutions flowed, so that the medium bathing the cytoplasmic side of the membrane patch could be rapidly changed. Four neighboring pipes were used for warm solutions and another four pipes were used for cold ones. The remaining two pipes were used for solutions at the reference temperature of 20°. Cold solutions were obtained by decreasing their temperature with a Peltier device; their temperature was measured by a sensor (type IT-23; Physitemp Instruments) placed in the liquid flowing through the pipe 1 mm in front of the termination of the pipe in the perfusing chamber. Warm solutions were obtained by heating the solutions. Similarly, their temperature was monitored by use of another sensor placed 1 mm in front of the termination of the pipe. Temperature changes were obtained by moving the patch pipette in the perfusing chamber in front of the selected pipe. The flow of solutions was regulated so as to have a good mechanical stability and a uniform temperature of cold and warm solutions within 0.5°C.

Liquid junction potentials

The voltage offset between the extracellular and intracellular sides of the membrane was routinely zeroed in the presence of a symmetrical solution on the two sides of the membrane at each different temperature. The liquid junction potential was −2 mV between a patch pipette filled with 110 mM NaCl and the bathing medium with 110 mM LiCl and less than 1 mV for all the other monovalent cations, and did not change by more than 2 mV when the temperature was varied between 30°C and 5°C. In these cases the liquid junction potential was not compensated, and the *I-V* relations were not corrected.

Determination of *I-V* relations

I-V relations were determined as described by Sesti et al. (1995). In the native channel the *I-V* relations obtained did not differ by more than 5% at any of the tested temperatures when going from 100 to 500 μM cyclic GMP, thus suggesting that in the presence of 100μM cyclic GMP the open probability of the cyclic GMP-activated channel was at its maximum level. Similarly, in the α subunit, the *I-V* relations obtained in the presence of 500 or 1000 μM were very similar when the temperature was varied between 5° and 30°C.

Estimation of the activation energy

The activation energy A_+ and (A^-) at 20°C was obtained by fitting the relation between the amplitude of the current flowing at +100 mV (and at −100 mV) and temperature with Eq. A1 of the Appendix. The current flowing at a given temperature was normalized to the current flowing at 20°C. The data were plotted on a semilogarithmic scale, and a straight line through the experimental points between 15° and 25° was obtained by a least-mean-square procedure. The slope of this straight line was taken as an estimate of the activation energy.

EXPERIMENTS

Determination of the activation energy in the native channel

According to the simple theory outlined in the Appendix, a possible way to estimate the activation energy is to measure the effect of temperature on the current flowing at very positive and negative membrane voltages and in the low activity range. Therefore, we have investigated the effect of temperature on the current flowing in the presence of a symmetrical concentration of the permeating ion.

Fig. 1 illustrates the effect of changing the temperature on the current carried by 50 mM Na^+ on both sides of a membrane patch excised from a rod outer segment. In Fig. 1 *A*, *I-V* relations obtained at different temperatures between 28° and 4°C are shown. The shape of the *I-V* relations was little affected when the temperature varied

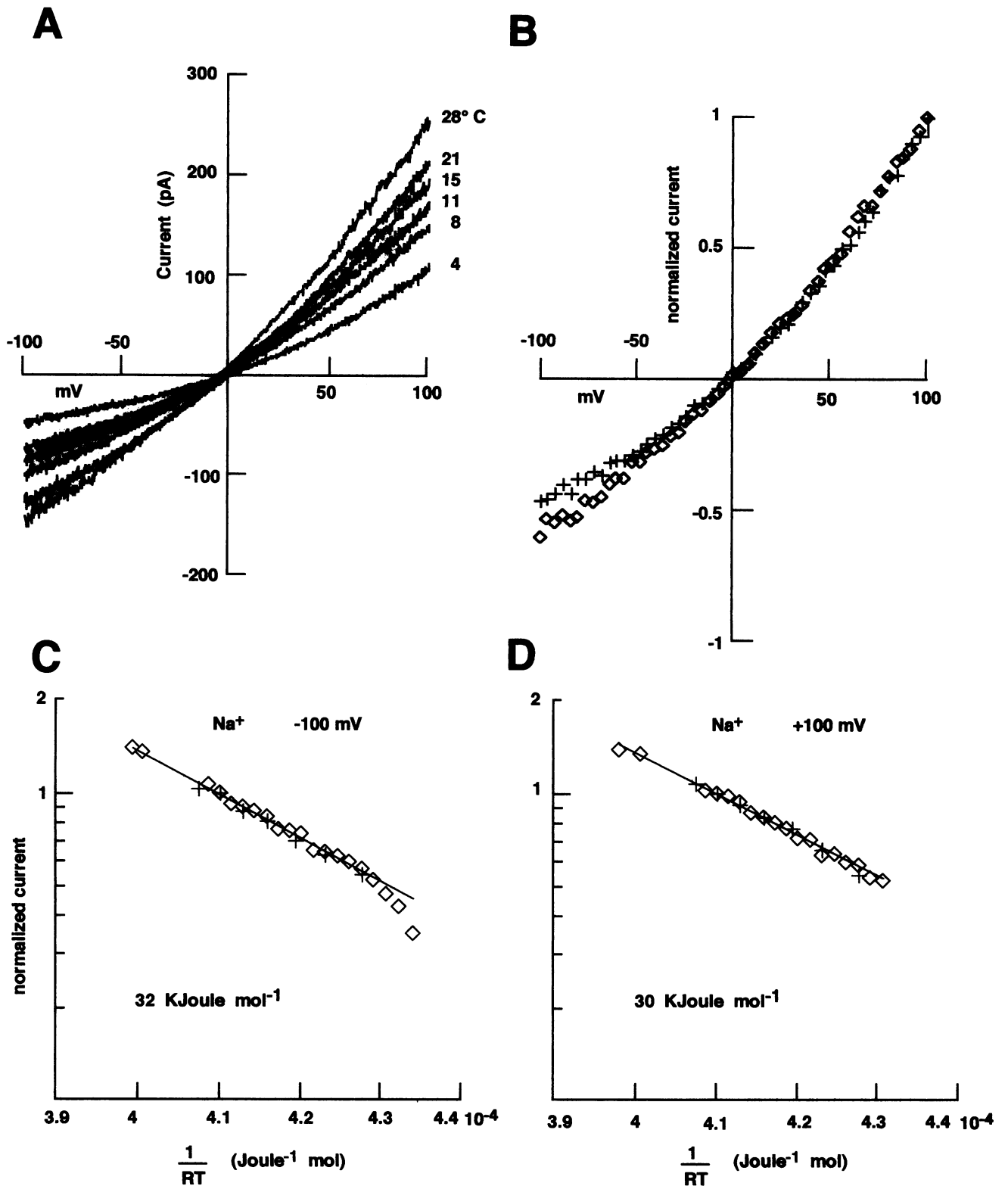

FIGURE 1 The effect of decreasing the temperature on the *I-V* relation in the presence of 50 mM symmetrical Na^+ in the native channel. (*A*) *I-V* relations at six different temperatures between 28° and 4°C. (*B*) *I-V* relations obtained at 22°C (◇) and 4°C (+) normalized to the current flowing at +100 mV. (*C*) The dependence of the current flowing at −100 mV on 1/*RT*. Data from two patches with the current normalized to the current flowing at 20°C. The straight line through the points indicates an activation energy of 32 kJ mol^{-1}. (*D*) As in *C*, but at +100 mV and with an activation energy of 30 kJ mol^{-1}.

between 15° and 25°C. However, when the temperature decreased below 10°C, some changes in the shape of the *I-V* relations could be observed, as illustrated in Fig. 1 *B*: the *I-V* relations had more outward rectifications at 4°C (+) than at 24°C (*diamonds*). Changes in the shape of the *I-V* relations observed when the temperature was decreased were not caused by changes of the equivalent electrical distances: at a temperature around 10°C the estimated value of the electrical distances (see Materials and Methods) for the different ions did not change significantly. Fig. 1, *C* and *D*, reproduces an Arrhenius plot for the current flowing at −100 and +100 mV, respectively. The straight line through the experimental points indicates an activation energy at 20°C of 32 and 30 kJ mol^{-1} at −100 and 100 mV, respectively. Below 5°C (i.e., for values of $1/RT$ larger than 4.25 10^{-4}) the activation energy of the macroscopic current increased sharply.

From these data it is evident that the macroscopic current flowing was halved when the temperature was decreased by about 15°C. Sesti et al. (1994) have reported that the estimated single-channel conductance of the native channel was halved when the temperature was decreased by 16°C. The reasonable agreement between these two measurements suggests that the effects of temperature on the amplitude of the macroscopic current and of the single-channel current are approximately similar.

As discussed in the Appendix, the relation between the barrier enthalpy and the activation energy (see Eqs. A25 and A26) was obtained under the hypothesis of the low activity range (see Eq. A6). It is useful to verify whether the estimation of the activation energy varies in the presence of different concentrations of the tested ion.

Fig. 2 reproduces families of *I-V* relations obtained at different temperatures in the presence of symmetrical amounts of 50 (Fig. 2 *A*) and 10 (Fig. 2 *B*) mM Li^+. The dependence of the current flowing at +100 mV on temperature in the presence of 50 and 10 mM symmetrical Li^+ is shown in Fig. 2, *C* and *D*, respectively. The activation energy in the presence of 50 and 10 mM Li^+ was 36 and 33.6 kJ mol^{-1}, respectively, and did not vary more that 10% in the presence of symmetrical solutions of Li^+ ranging from 2.5 to 110 mM.

The macroscopic current was halved when the temperature was reduced by 14.5°, 14°, and 12.5° for K^+, Rb^+, and Cs^+, respectively, and the activation energy was 31.8, 34.5, and 41.3 kJ mol^{-1} for the same ions. The shape of the *I-V* relations did not change significantly for any of the tested ions when the temperature varied between 15° and 25°C. For Cs^+, Li^+, and K^+, no changes were observed between 5° and 25°C, but for Na^+, Rb^+, and, to a lesser extent, for NH_4^+ as well, a larger outward rectification was observed when the temperature decreased below 10°C. Collected data for the activation energy at +100 and −100 mV for the various ions are reported in Table 1. The activation energy in the presence of symmetrical solutions of 2.5 and 50 mM was very similar for all alkali monovalent cations and NH_4^+.

TABLE 1 The activation energy at +100 (A^+) and −100 mV (A^-) for the native channel and the α subunit

	A^+ (kJ mol^{-1})	$A^+_{s.c.}$ (kJ mol^{-1})	A^- (kJ mol^{-1})
Native channel			
NH_4^+	22.4 ± 1.7		22.9 ± 1.6
Li^+	35.8 ± 1.8		36.8 ± 1.7
Na^+	30 ± 1.9		32.2 ± 2
K^+	31.8 ± 1.7		31 ± 1.5
Rb^+	34.5 ± 1.8		36.3 ± 1.6
Cs^+	41.3 ± 2.1		40.8 ± 2.1
Alpha subunit			
NH_4^+	38.9 ± 3.2	33 ± 2.3	35 ± 2.1
Li^+	45.2 ± 4.3		49.4 ± 3.2
Na^+	38.2 ± 3.5	40.4 ± 3.5	43.3 ± 2.8
K^+	37.5 ± 2.7		45.3 ± 3
Rb^+	47.3 ± 4		50.1 ± 2.9
Cs^+	49.4 ± 3		53.2 ± 1.9

$A^+_{s.c.}$ is the activation energy of a single channel and was measured for the Na^+ and NH_4^+ at +100 mV in the α subunit. The activation energies were obtained from Eq. A1 and the procedure illustrated in Materials and Methods.

The sequence of the activation energy of the native channel at +100 mV is

$$A_{NH_4^+} < A_{Na^+} \sim A_{K^+} < A_{Rb^+} < A_{Li^+} < A_{Cs^+}. \quad (1)$$

This sequence is not the reverse of the permeability sequence based on the reversal potential, because Li^+ has a higher activation energy than Na^+. Therefore, ionic selectivity does not appear to be uniquely determined by the activation energy, i.e., by enthalpic contributions, and it is important to investigate whether different ions have a different entropic term.

The effect of temperature on the reversal potential of biionic solutions in the native channel

As shown in the Appendix and discussed by Miller et al. (1988), a possible way to estimate the contribution of entropic factors to the determination of the ionic selectivity is to analyze the dependence of the reversal potential on temperature.

Fig. 3 illustrates the effect of varying the temperature on the reversal potential between Na^+ and Li^+ in the native channel. In these experiments the reversal potential v_{rev} was determined from *I-V* relations obtained with voltage ramps between −20 and +20 mV. Each *I-V* relation was obtained as the average of at least five individual voltage ramps. Fig. 3, *A* and *C*, reproduce *I-V* relations obtained at two different temperatures and when the patch pipette was filled with 110 mM Na^+ and Li^+, respectively. At about 20°C, when Na^+ was present in the patch pipette, the reversal potential was about −4 mV; when Li^+ was in the patch pipette v_{rev} was about +3.5 mV. From the *I-V* relations shown in Fig. 3, *A* and *C*, it is evident that when the temperature decreased by about 15°C, the reversal potential approached a value near 0 mV. Fig. 3, *B* and *D*, reproduces data collected from two

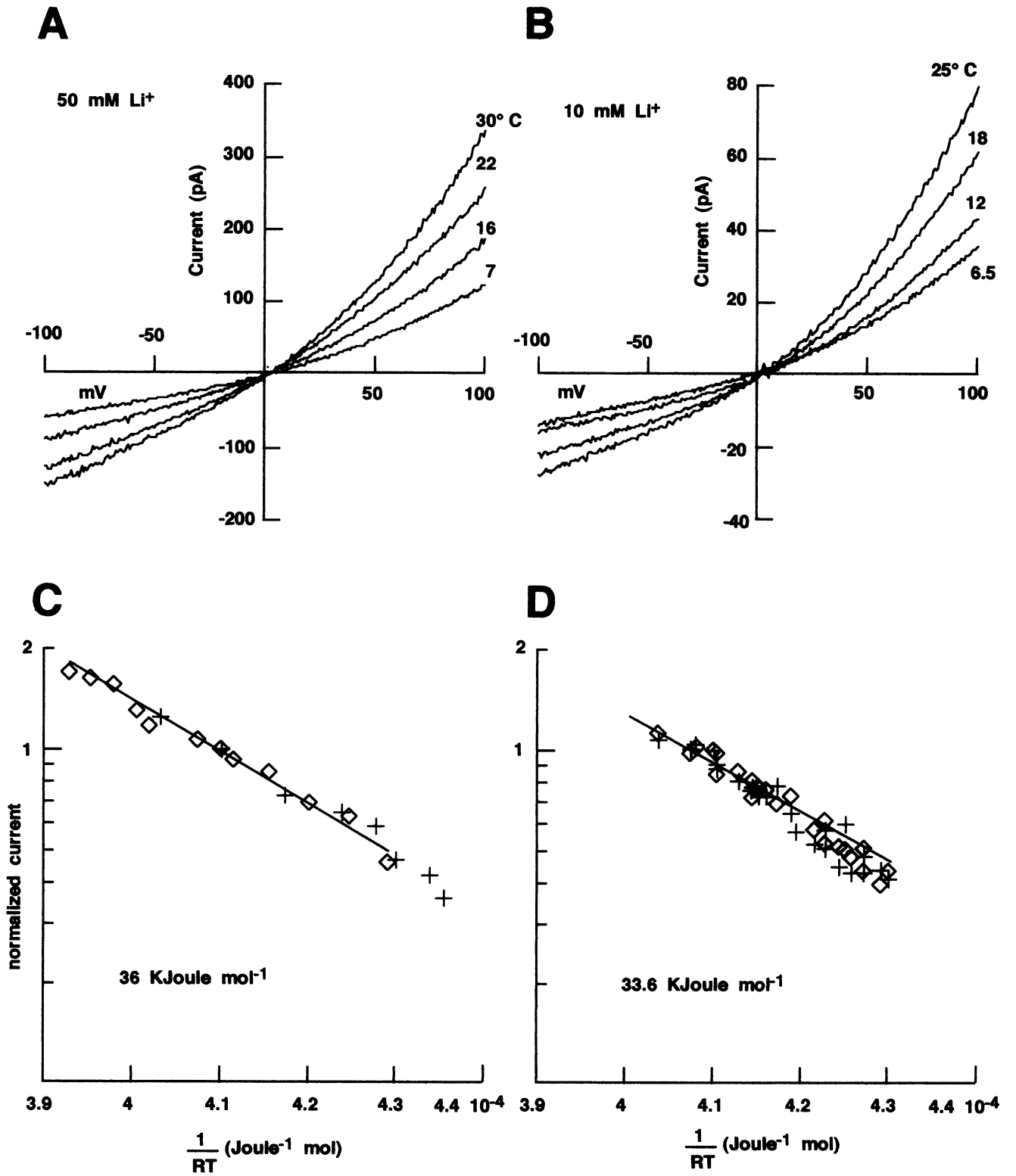

FIGURE 2 The effect on the *I-V* relation of decreasing the temperature in the presence of 50 (*A*) and 10 (*B*) mM symmetrical amounts of Li^+ in the native channel. Each *I-V* relation was obtained as the average of at least three voltage ramps. (*C* and *D*) The dependence of the current flowing at +100 mV in the presence of 50 (*C*) and 10 (*D*) mM symmetrical Li^+ on 1/*RT*. In each panel different symbols indicate different patches with the current normalized to the current flowing at 20°C. The straight line through the points in *C* and *D* indicate an activation energy of 36 and 33.6 kJ mol^{-1} in the presence of 50 and 10 mM Li^+.

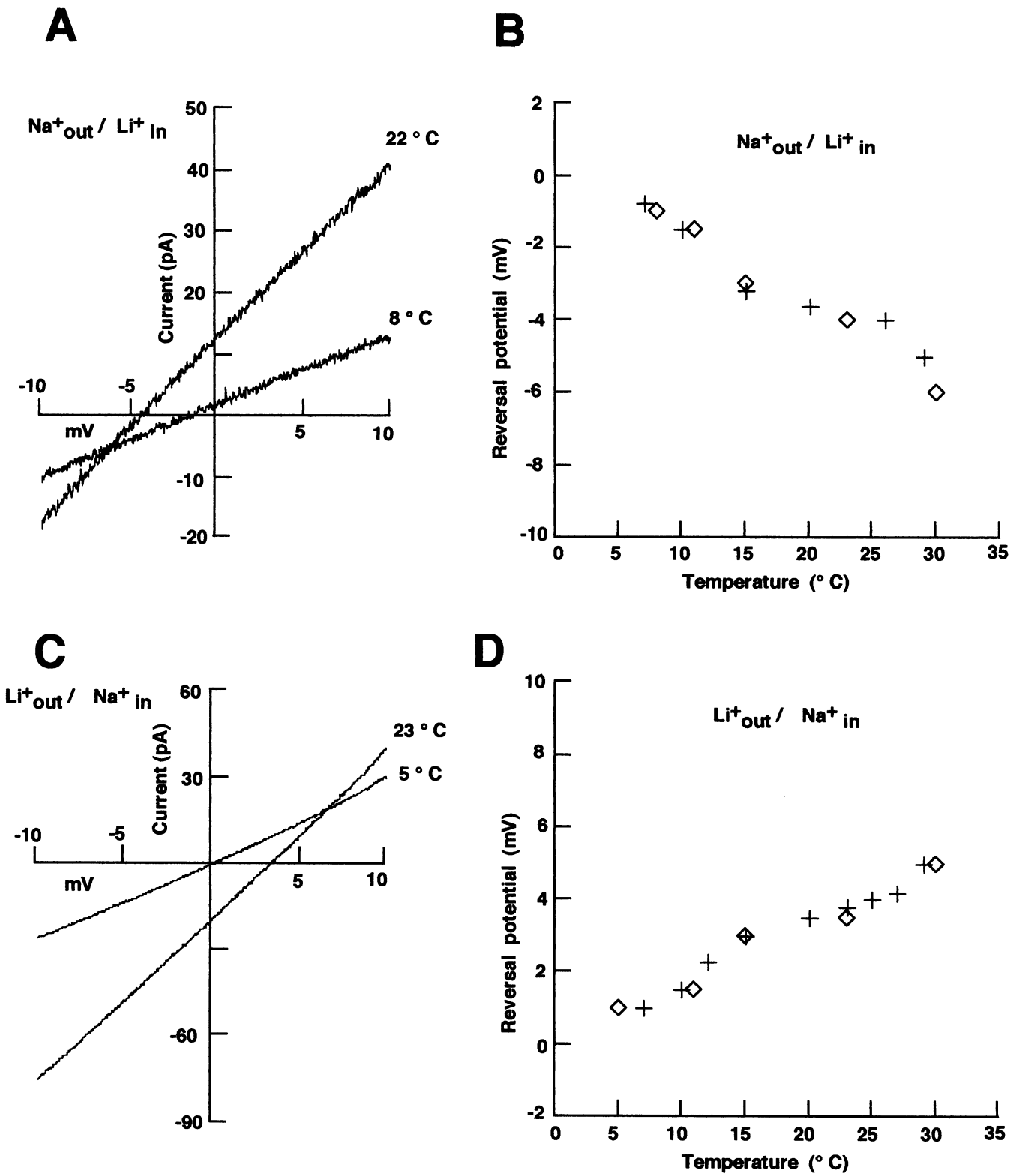

FIGURE 3 The dependence of the reversal potential of biionic solutions of Na^+ and Li^+ on temperature in the native channel. (*A*) *I-V* relations at two different temperatures in the presence of 110 mM Na^+ in the patch pipette and 110 mM Li^+ in the bathing medium. (*B*) Dependence of the reversal potential on the temperature in two patches. (*C*) *I-V* relations at two different temperatures in the presence of 110 mM Li^+ in the patch pipette and 110 mM Na^+ in the bathing medium. (*D*) Dependence of the reversal potential on the temperature in two patches. Each *I-V* relation in *A* and *C* was the average of at least five voltage ramps.

TABLE 2 The reversal potential (v_{rev}) and the effect of temperature on v_{rev} (dv_{rev}/dT) for the native channel and the α subunit at varying osmolarity

	v_{rev} (mV)			dv_{rev}/dT (mV/°C)		
	2.5	50	110	2.5	50	110 Osmolarity
Native channel						
NH_4^+	n.a.	−25 ± 3	−26 ± 4	n.a.	0.32 ± .1	0.38 ± 1.2
Li^+	−1 ± 1.	−4 ± 1.	−4 ± 1.5	−0.1 ± 0.1	−0.22 ± 0.05	−0.2 ± 0.07
Na^+	—	—	—	—	—	—
K^+	1 ± 1	0 ± 1.5	0.5 ± 1	0.01 ± 0.02	0.01 ± 0.01	0.01 ± 0.015
Rb^+	n.a.	8 ± 2	9 ± 3	n.a.	−0.07 ± 0.03	−0.09 ± 0.05
Cs^+	n.a.	17 ± 3	16 ± 4	n.a.	−0.33 ± 0.	−0.3 ± 0.05
α subunit						
	2.5	50		2.5	50 Osmolarity	
NH_4^+	−22 ± 4	−28 ± 4		0.2 ± 0.15	0.3 ± 0.1	
Li^+	0.1 ± 0.1	8 ± 1.5		−0.1 ± −.1	−0.2 ± 0.08	
Na^+	—	—		—	—	
K^+	0 ± 1.5	+1 ± 1		0.1 ± 0.1	0.02 ± 0.05	
Rb^+	10.4 ± 2	15.3 ± 3		−0.1 ± 0.15	−0.2 ± 0.05	
Cs^+	13.5 ± 2.5	25 ± 4		−0.15 ± 0.2	−0.35 ± 0.1	

v_{rev} is referred to a biionic solution with Na^+ inside the patch pipette. The osmolarity was 2.5, 50, and 110 mM for the native channel and 2.5 and 50 for the α subunit. n.a., not available.

patches. There was no noticeable difference, regardless of whether Li^+ was at the inside or at the outside of the membrane patch, and in both cases the selectivity of the cGMP-activated channel for Li^+ over Na^+ was decreased and almost abolished when the temperature was reduced to near 0°C.

These results clearly show that the selectivity between Na^+ and Li^+ based on the reversal potential is highly dependent on temperature and can be abolished by decreasing the temperature to around 0°C. This effect is consistent with a substantial entropic contribution to the selectivity between Na^+ and Li^+ observed at room temperature. In experiments in which 50 mM Li^+ was present in the bathing medium and an equivalent amount of the other ions was present in the patch pipette, the reversal potential between Li^+ and NH_4^+ or K^+ or Rb^+ increased when the temperature was decreased. Only in the presence of Cs^+ did the reversal potential decrease when the temperature was reduced. It is useful to quantify the change of the reversal potential with temperature by evaluating the quantity dV_{rev}/dT. This quantity is reported in Table 2 for the different ions. Very similar results were obtained when the concentration of the two ionic species under investigation was 50 or 110 mM or when the reference ion was in the patch pipette and not in the bathing medium.

It has been shown recently that the low activity range in both the native and w.t. cGMP-gated channels is below 10 mM (Sesti et al., 1995), and it is useful to examine the effect of changing the temperature on the reversal potential of biionic solutions in the low activity range. When the patch pipette was filled with 2.5 mM NaCl and an equimolar amount of LiCl was in the bathing solution, the reversal potential was −2±1 mV and the value of dv_{rev}/dT was −0.1 mV/°C. Similar values were obtained when K^+ replaced Na^+.

The effect of temperature on the single-channel current of the α subunit

Given the very short open time of the native channel (Sesti et al., 1994), it is difficult to measure reliably the effect of varying the temperature on the single-channel current, and accurate measurements can be made only on the macroscopic current. As the α subunit of the w.t. cyclic GMP-gated channel has a much longer open time, it is possible to measure its single-channel current reliably (Nizzari et al., 1993). Therefore, we have investigated the effect of varying the temperature on the current flowing through cyclic GMP-gated channels excised from the membrane of oocytes previously injected with the mRNA encoding for the w.t. channel.

Fig. 4 *A* illustrates current recordings from a patch containing a single channel activated by 100μM cyclic GMP in the presence of a symmetrical solution with 110 mM NH_4^+ at different temperatures, ranging between 10° and 27°C. At 27° and 22°C channel openings and closings were very rapid, and well-resolved square events were only occasionally observed. At 16° and 19°C transitions between the closed and open states became significantly slower, and well-resolved openings could be clearly observed. When the temperature was decreased to 10°C the single-channel current became rather small, and channel openings were reduced, indicating that the open probability had decreased. Fig. 4, *B* and *C*, reproduces amplitude histograms of single-channel currents at 27° and 16°C from the current record-

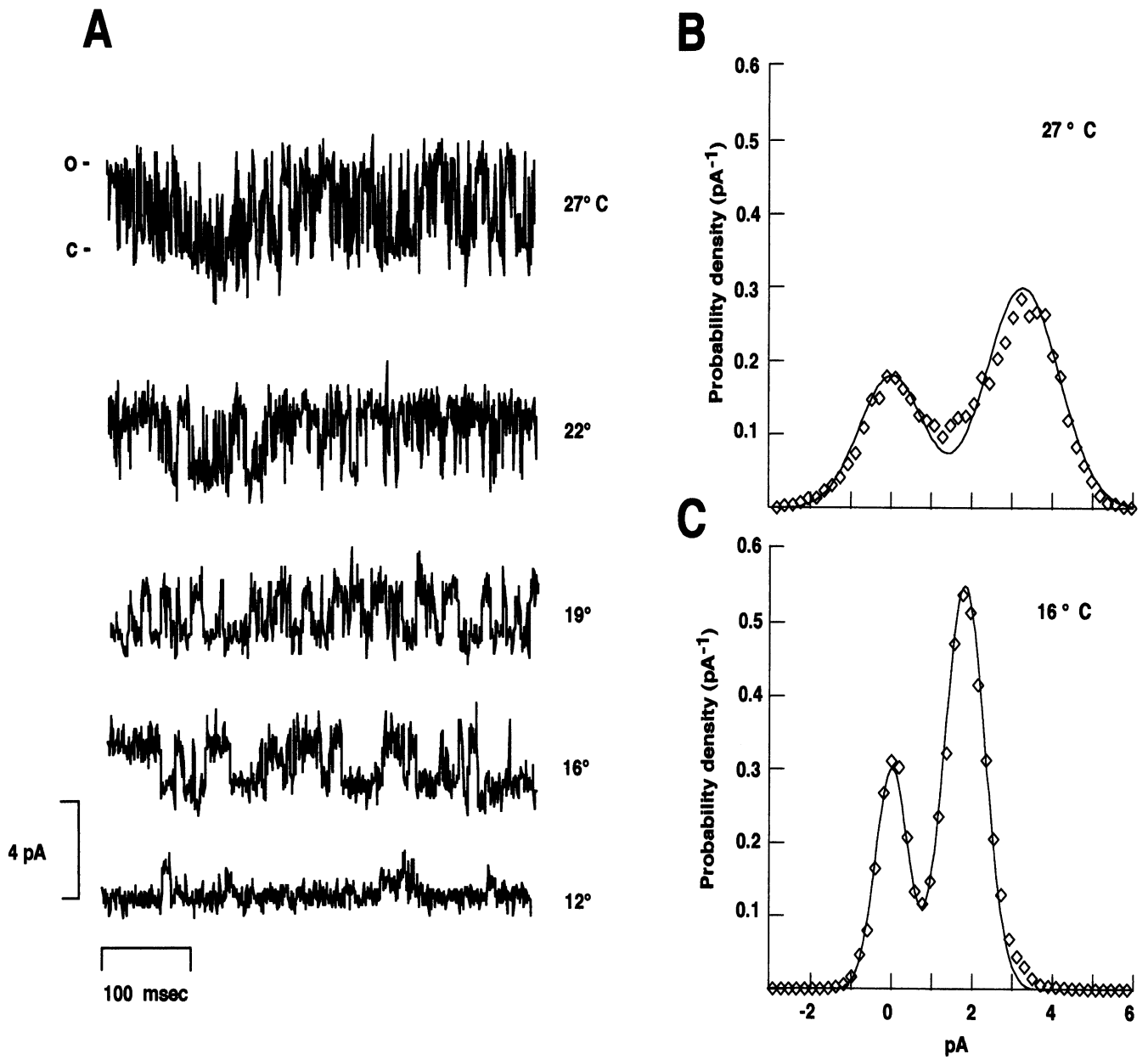

FIGURE 4 The effect of temperature on the single-channel properties of the w.t. channel. (*A*) Single-channel recordings from a patch containing a single channel. Membrane voltage was held at +100 mV in the presence of 110 mM NH_4^+ at both sides of the membrane patch. The channel was activated by 500μM cyclic GMP. Each trace was filtered at 2 kHz and sampled at 6 kHz and recorded at the temperature indicated. (*B* and *C*) Amplitude histograms of current amplitudes at 27° and 16°C. Theoretical curves obtained with the equation $a_1 e^{(-x^2/2\sigma_c^2)} + a_2 e^{-(x-i_{sc})^2/2\sigma_o^2}$, where i_{sc} is the single-channel current, σ_c and σ_o are the standard deviations of the closed and open state, respectively, and a_1 and a_2 are appropriate scaling constants. The values for i_{sc}, σ_c^2, σ_o^2, a_1 and a_2 were 3.25 pA, 0.8 pA^2, 0.9 pA^2, 0.18 pA^{-1}, and 0.31 pA^{-1} in *B* and 1.8 pA, 0.4 pA^2, 0.5 pA^2, 0.3 pA^{-1}, and 0.58 pA^{-1} in *C*.

ings shown in Fig. 4 *A*. These histograms were normalized to a unit area and could be fitted as the sum of two Gaussian distributions (*continuous line*) centered around the closed and open levels, which was 3.25 and 1.8 pA at 27° and 16°C, respectively. The area of the Gaussian distribution centered around the open level was taken as a measure of the open probability, which, in the case of the histograms of Fig. 4, *B* and *C*, was 0.65 and 0.72, respectively.

Fig. 5, *A* and *B*, illustrates the dependence of the single-channel current on temperature, at +100 mV and in the presence of a symmetrical solution containing 110 mM NH_4^+ and Na^+, respectively. The straight lines through the points indicate an activation energy of 33 and 40.4 kJ/M for NH_4^+ and Na^+, respectively. Fig. 5 *C* reproduces the dependence of the open probability when the temperature was varied between 8° and 27°C in the presence of 100 μM cyclic GMP at +100 mV. These data were obtained from two single-channel recordings in the presence of 110 mM NH_4^+ and one in the presence of 110 mM Na^+. The open probability did not change significantly when the tempera-

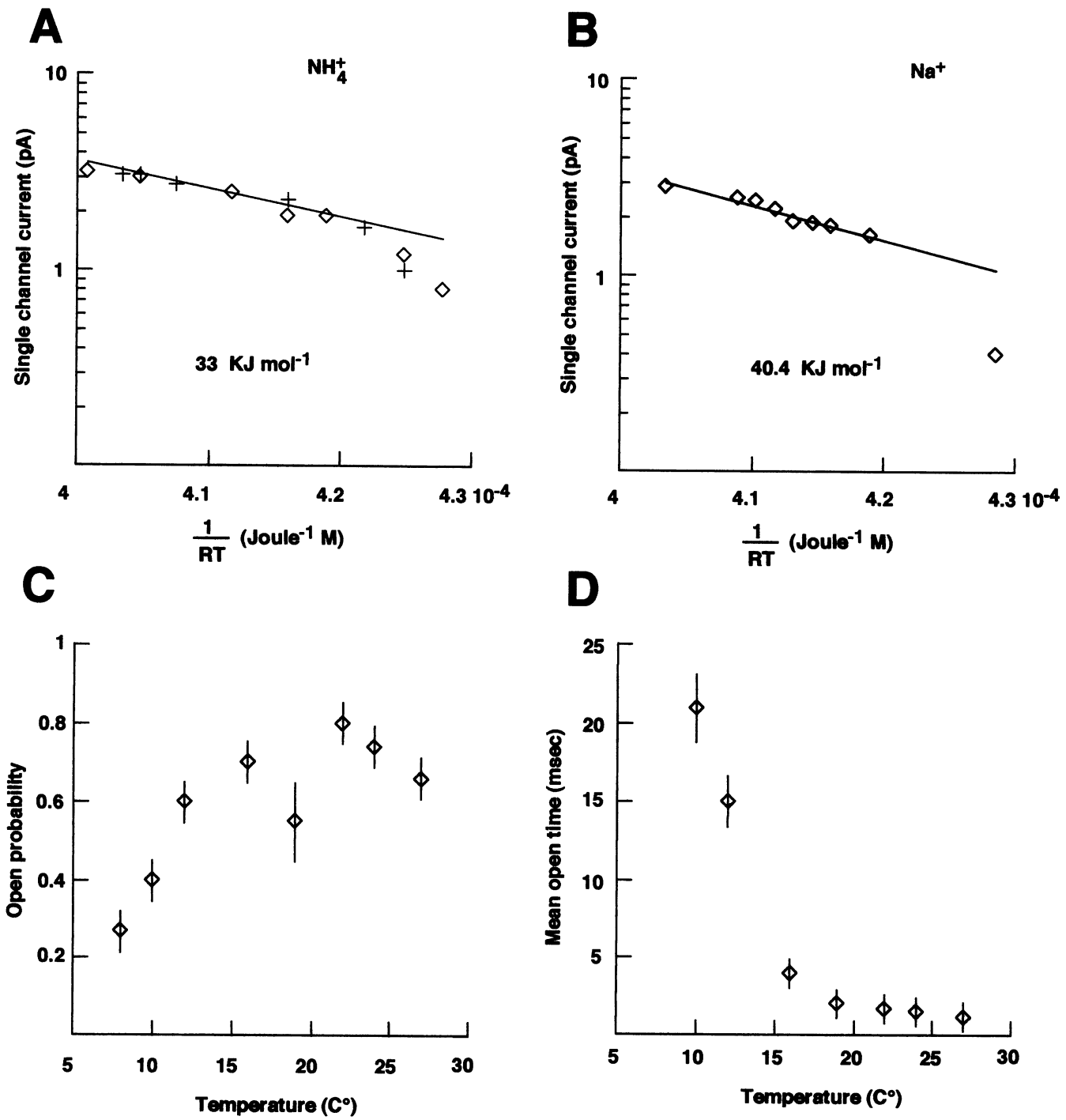

FIGURE 5 The dependence of single-channel properties of the w.t. channel on temperature. (*A* and *B*) Dependence of the single-channel current on temperature in the presence of 110 mM NH_4^+ and Na^+, respectively. The straight lines through the points indicate an activation energy of 33 and 40.4 kJ mol^{-1}, respectively. (*C*) Dependence of the open probability on the temperature in the presence of 100μM cyclic GMP. Average values from two patches in the presence of 110 mM NH_4^+ and one patch in the presence of 110 mM Na^+. The closed probability P_c was computed as the area of the Gaussian distribution $a_2 e_c^{-x^2}/2\sigma^2$ and the open probability P_o as $1 - P_c$. (*D*) Dependence of the mean open time on temperature. The mean open time was obtained by analyzing single-channel recordings with the IPROC program and is the mean of both short and long openings (see Nizzari et al., 1993).

ture was varied between 16° and 27°C and decreased when the temperature was reduced below 14°C. As shown in Fig. 5 *B*, the mean open time was about 1 ms at 27° and increased to about 20 ms when the temperature was reduced to about 10°.

The effect of temperature on the macroscopic current through the α subunit

The single-channel current through the w.t. carried by Li^+, Rb^+, and Cs^+ at +100 mV is less than 1 pA (Nizzari et al.,

1993), and it is rather difficult to determine the activation energy of the single-channel current for these ions. Therefore, we have analyzed the effect of temperature on the macroscopic current through the α subunit of the channel.

Fig. 6, *A* and *B*, illustrates the effect of varying the temperature from 8° to 25°C on the macroscopic current activated by 100μM cyclic GMP in symmetrical solutions containing 50 mM NH_4^+ and Rb^+, respectively. The shape of the *I-V* relation obtained from the α subunit did not have the outward rectification characteristic of the native channel (data not shown). The shape of the *I-V* relations in the presence of NH_4^+ did not change significantly when the temperature was reduced. In contrast, in the presence of Rb^+ (and Cs^+) decreasing the temperature reduced the current flowing at +100 mV more strongly than that flowing at −100 mV (see Fig. 9 *B*). At temperatures below 10° the *I-V* relations in the presence of a symmetrical concentration of 50 mM Rb^+ or Cs^+ had a strong inward rectification. The dependence of the macroscopic current carried by 50 mM NH_4^+ and Rb^+ at +100 mV on temperature is shown in Fig. 6, *C* and *D*. The straight lines through the points indicate an activation energy of the macroscopic current of 32.1 and 47.5 kJ mol^{-1} for NH_4^+ and Rb^+, respectively. Very similar results were obtained when symmetrical solutions containing 110 mM were used. The activation energies of the macroscopic current carried by the other ions at +100 and −100 mV are reported in Table 1. The activation energies of the single-channel current and the macroscopic current in the presence of Na^+ or NH_4^+ were very similar, in agreement with the observation that the open probability did not change appreciably when the temperature was varied between 15° and 25°C.

The effect of temperature on the reversal potential of biionic solutions in the α subunit

The ionic selectivity based on the reversal potential is different in the native and in the w.t. cyclic GMP-activated channel (Kaupp et al., 1989; Nizzari et al., 1993; see also Table 2). Table 2 reports the values of the reversal potentials at 20°C for the biionic solutions in the w.t. channel, when 50 mM Li^+ was in the bathing medium and an equimolar amount of the cation X^+ was in the patch pipette.

The major difference between these reversal potentials and those measured in the native channel is related to Na^+, K^+, and Li^+. The native channel is more selective to Li^+ than to Na^+ and K^+, whereas the opposite effect is observed in the w.t. channel. To better understand these differences, it is useful to also evaluate the effect of temperature on the reversal potential of biionic solutions in the w.t. channel.

Fig. 7 illustrates the effect of varying the temperature on the reversal potential when the patch pipette contained 50 mM NH_4^+ and the bathing medium contained an equimolar amount of Li^+ (Fig. 7 *A*) or Na^+ (Fig. 7 *B*). Fig. 7, *A* and *C*, shows *I-V* relations at different temperatures. In the presence of Na^+ in the bathing medium the reversal potential v_{rev} was 19 mV at 29°C and increased to 28 mV at 5°C. Similarly, in the presence of Li^+, the reversal potential increased from 27 to 47 mV when the temperature was decreased from 29° to 5°C. The dependence of the reversal potential on temperature with 50 mM Li^+ or Na^+ present in the patch pipette is illustrated in Fig. 7, *C* and *D*, respectively. The values of the reversal potential in Fig. 7, *C* and *D*, were obtained with 50 mM Li^+ (*circles*), Na^+ (*diamonds*), K^+ (+), Rb^+ (*squares*), Cs^+ (X), and NH_4^+ (*triangles*) in the bathing medium. As in the case of the native channel, it is useful to quantify the effect of temperature on the reversal potential for the w.t. channel as well, by evaluating the quantity dv_{rev}/dT. Table 2 reports the values of dv_{rev}/dT when 50 mM Na^+ was present inside the bathing medium.

The effect of temperature in the low activity range

The previous analysis of the effect of temperature on the macroscopic current and on the reversal potential was obtained at the ionic activity of 50 mM. As the low activity range for the native and w.t. channels is likely to be smaller than 50 mM (see Sesti et al., 1995), it is useful to repeat these experiments at a much lower ionic activity. As for the native channel, the activation energy of the macroscopic current through the w.t. channel in the presence of symmetrical concentrations of 50 and 2.5 mM was approximately the same. When the effect of temperature on the reversal potential was analyzed with symmetrical biionic solutions containing 2.5 mM permeant cations, the reversal potentials were similar, but not identical, to those observed in the presence of biionic solutions of 50 mM. As shown in Table 2, the ionic selectivity based on the reversal potential was less pronounced, and the values obtained for dv_{rev}/dT were affected by a significantly larger variability.

The ionic selectivity of mutant channels

It has been shown that glutamate 363 of the w.t. cyclic GMP-activated channel controls many features of ionic permeation (Root and MacKinnon, 1993; Eismann et al., 1994; Sesti et al., 1995; Park and MacKinnon, 1995). Therefore, it is useful to analyze the ionic selectivity of mutant channels where glutamate 363 has been replaced with a different amino acid.

Table 3 illustrates collected data on the reversal potential for alkali monovalent cations for the w.t. and mutant channels E363D, E363N, E363Q, E363S, E363A, and E363G. It is evident that when glutamate in position 363 was neutralized and replaced with a glutamine, the permeability sequence based on the reversal potential remained largely unaltered. In contrast, when glutamate 363 was replaced with a smaller neutral amino acid, such as serine, alanine, or glycine, the ionic selectivity was significantly modified and large alkali cations, such as Rb^+ and Cs^+, became more

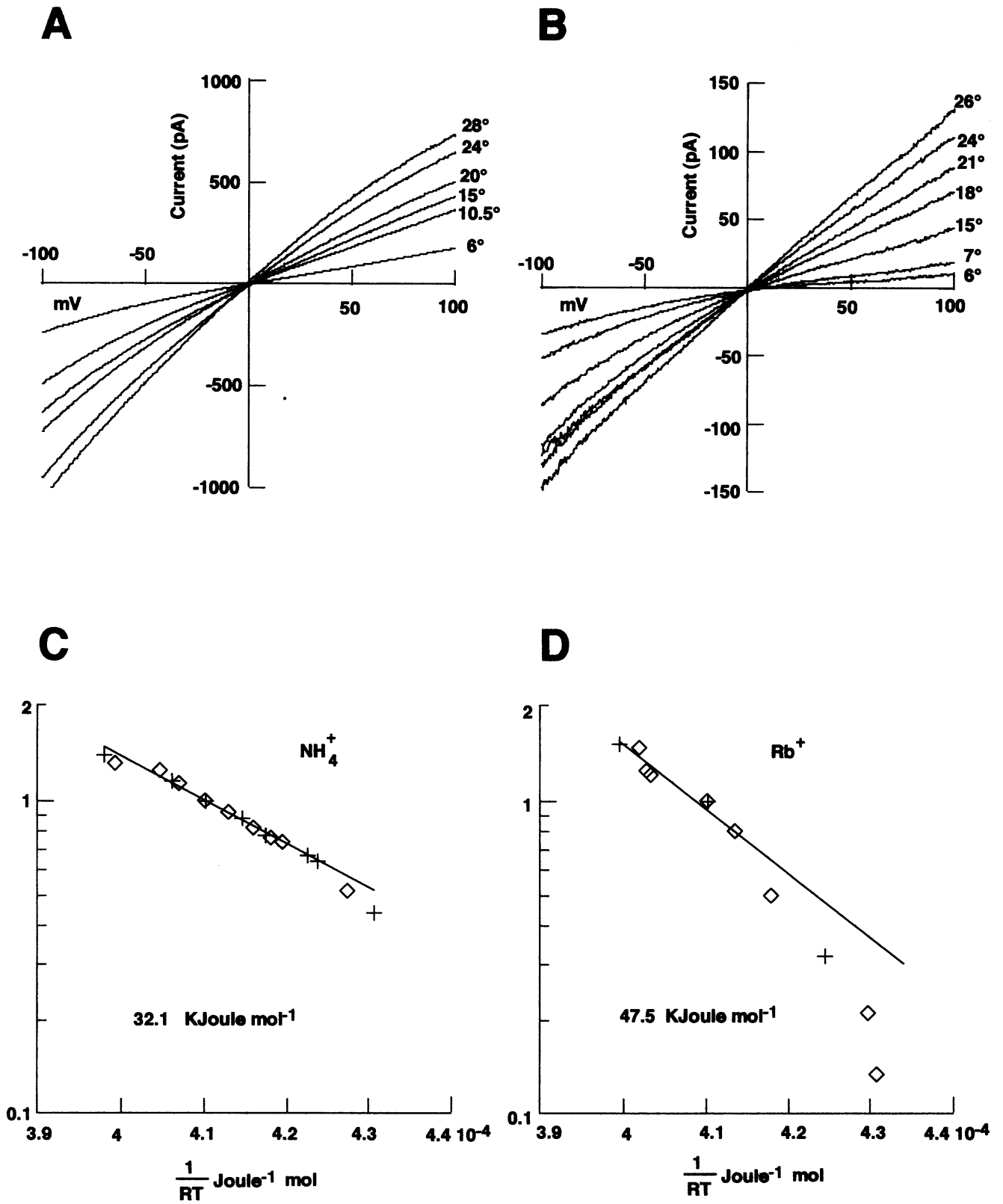

FIGURE 6 The effect on the *I-V* relation of decreasing the temperature of the w.t. channel. (*A* and *B*) *I-V* relations at different temperatures in the presence of 50 mM NH_4^+ and Rb^+, respectively. (*C* and *D*) Dependence of the current flowing at +100 mV on $1/RT$ in the presence of 50 mM NH_4^+ and Rb^+, respectively. The straight lines through the points in *C* and *D* indicate an activation energy of 32.1 and 47.5 kJ mol^{-1}, respectively.

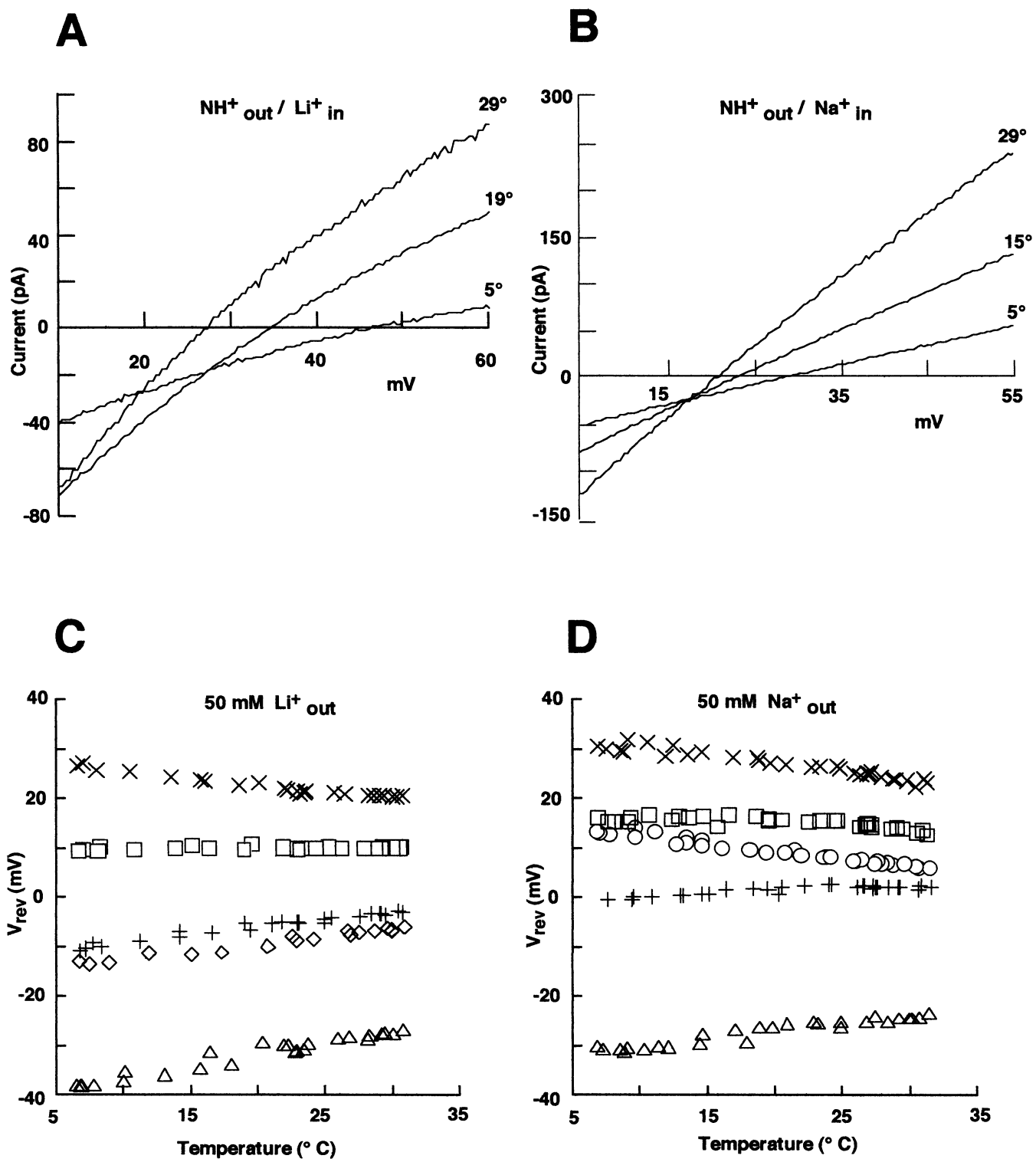

FIGURE 7 The dependence of the reversal potential of biionic solutions on temperature in the w.t. channel. (*A* and *B*) *I-V* relations at three different temperatures in the presence of 50 mM NH_4^+ in the patch pipette and 50 mM Na^+ and Li^+ in the bathing medium, respectively. (*C* and *D*) Dependence of the reversal potential on the temperature in the presence of 50 mM Li^+ (*C*) and Na^+ (*D*) in the patch pipette and an equimolar amount of Li^+ (○), Na^+ (◇), K^+ (+), Rb^+ (□), Cs^+ (X), and NH_4^+ (△).

permeable. The ionic selectivity of mutant channels E363S, E363A, and E363G became similar to that of ions free to diffuse in water, suggesting that the ionic radius of mutant channels at the selectivity filter may have significantly increased. To test this hypothesis, the ionic permeation of large organic cations through the w.t. and mutant channels

TABLE 3 Reversal potential of w.t. and mutant channels in biionic solutions with 110 mM Na^+ in the patch pipette and an equimolar amount of alkali cations in the bathing medium

	Li^+	K^+	Rb^+	Cs^+
w.t.	7.5 ± 3.1	1 ± 1.3	8.2 ± 3.1	26.3 ± 4.2 mV
E363D	14.8 ± 2.9	1.5 ± 1.2	6 ± 3.2	16.3 ± 3.4
E363N	8.7 ± 2.1	−7 ± 2.3	−6 ± 3.2	2 ± 1.2
E363Q	5.5 ± 2.8	1 ± 1.2	6 ± 2.1	21 ± 3.3
E363S	8.3 ± 1.9	−9.8 ± 3.4	−9.8 ± 2.1	1.2 ± 3.2
E363A	6.2 ± 2.6	−8.3 ± 2.2	−8.5 ± 1.9	−2.2 ± 3.3
E363G	8.3 ± 2.8	−8.1 ± 3.2	−8.5 ± 2.3	−2.4 ± 2.5

Each value was obtained from at least five different patches (mean ± SD).

can be analyzed. Diethylammonium (the dimensions of which are 4.9 × 5.4 × 7.3 Å), which is not permeable through the w.t. channel, has been shown to become permeable through the mutant E363S (Bucossi et al., 1996). Trimethylammonium (the dimensions of which are 4.0 × 5.4 × 6.0 Å) is not permeable through the native cGMP-gated channel from larval tiger salamander rods (Picco and Menini, 1993) but is permeable through the w.t. channel from bovine rods (Bucossi et al., 1996), suggesting that the size of the narrowest area of the pore is larger in the w.t. channel than in the native channel. By repeating the same experiments of Bucossi et al. (1996) it is possible to show that mutant channel E363G is also permeable to triethylammonium, the dimensions of which are 5.1 × 6.2 × 7.3 Å. These data indicate that the narrowest section of the pore of the w.t. channel is about 4.0 × 5.4 Å, whereas that of the mutant channels E363S and E363G is about 4.9 × 5.4 Å and 5.1 × 6.2 Å, respectively.

The ionic permeation through the mutant channel E363G

To understand the mechanisms underlying the changes in the ionic selectivity (see Table 3) when glutamate 363 is mutated to an amino acid with a smaller residue, it may be useful to analyze in detail the ionic permeation through the mutant channel E363G, as glycine is the smallest amino acid residue. In particular, the determination of the enthalpic and entropic contributions of the mutant channel E363G to the ionic selectivity can be useful to clarify the physical mechanisms underlying the selectivity changes described in Table 3. Therefore, the effect of temperature on the ionic permeation was analyzed as in the case of the native and w.t. channels.

When the temperature was decreased from 22° to 10°C, the macroscopic current carried by Na^+ and other alkali cations increased at both −100 and +100 mV. This behavior was not observed in either the native or the w.t. channel. Indeed, in the w.t. channel, the macroscopic current was almost halved when the temperature was decreased from 22° to about 10°C. As a consequence, it is necessary to analyze the effect of temperature at a single-channel level and to separate the influence of temperature on the single-channel conductance and on the open probability. Fig. 8 *A* illustrates current recordings at three different temperatures from a patch containing at least three copies of the mutant channel E363G in the presence of a symmetrical solution of 500 mM Na^+ at +60 mV. At 27°C the open probability was so small that almost no multiple openings occurred, which became evident only when the temperature was reduced to 20°C or 10°C. At 27°C, the channel openings were very brief and often could not be completely resolved. Amplitude histograms at two different temperatures are shown in Fig. 8 *B*. The analysis of amplitude histograms indicates that, at 20°C, the single-channel current was about 2.5 pA and the open probability was about 0.03. At 10°C, the single-channel current decreased to 1.45 pA, but the open probability increased to 0.12. Fig. 8 *C* shows the dependence of the single-channel current on temperature; the straight line through the points indicates an activation energy of 38.3 kJ mol^{-1}. For the other alkali cations the activation energy at the single-channel level was 41 ± 3, 28.2 ± 2.5, 30 ± 2.8, and 28.5 ± 3 kJ mol^{-1} for Li^+, K^+, Rb^+, and Cs^+, respectively. Thus the sequence of the activation energy for the mutant channel E363G is

$$A_{Li} > A_{Na} > A_{K^+} \sim A_{Cs^+} \sim A_{Rb^+}. \quad (2)$$

This sequence is rather different from that measured in the w.t. channel, where Na^+ is the ion with the lowest activation energy. The dependence of the open probability on temperature is shown in Fig. 9 *D*; it is evident that the open probability increased significantly when the temperature was reduced.

Fig. 9, *A*, *B*, and *C*, shows *I-V* relations of the mutant channel E363G at 9°C, 20°C, and 27°C, respectively. These *I-V* relations were obtained in the presence of 110 mM Na^+ in the patch pipette and equimolar amounts of Na^+ (*diamonds*), Li^+ (*circles*), Rb^+ (*squares*), and Cs^+ (X) in the bathing medium. At 9°C, the reversal potential was +8, −10, and −5 mV for Li^+, Rb^+, and Cs^+, respectively. At 27°C, these values were +6, −4.5, and −1 mV. Fig. 9 *D* illustrates the dependence of the reversal potential on temperature for biionic solutions of Li^+ (*circles*), Rb^+ (*squares*), and Cs^+ (X) in the presence of 110 mM Na^+ in the patch pipette. The value of dv_{rev}/dT was −0.13, 0.3, and 0.22 for Li^+, Rb^+, and Cs^+, respectively. These results indicate that the ionic selectivity of

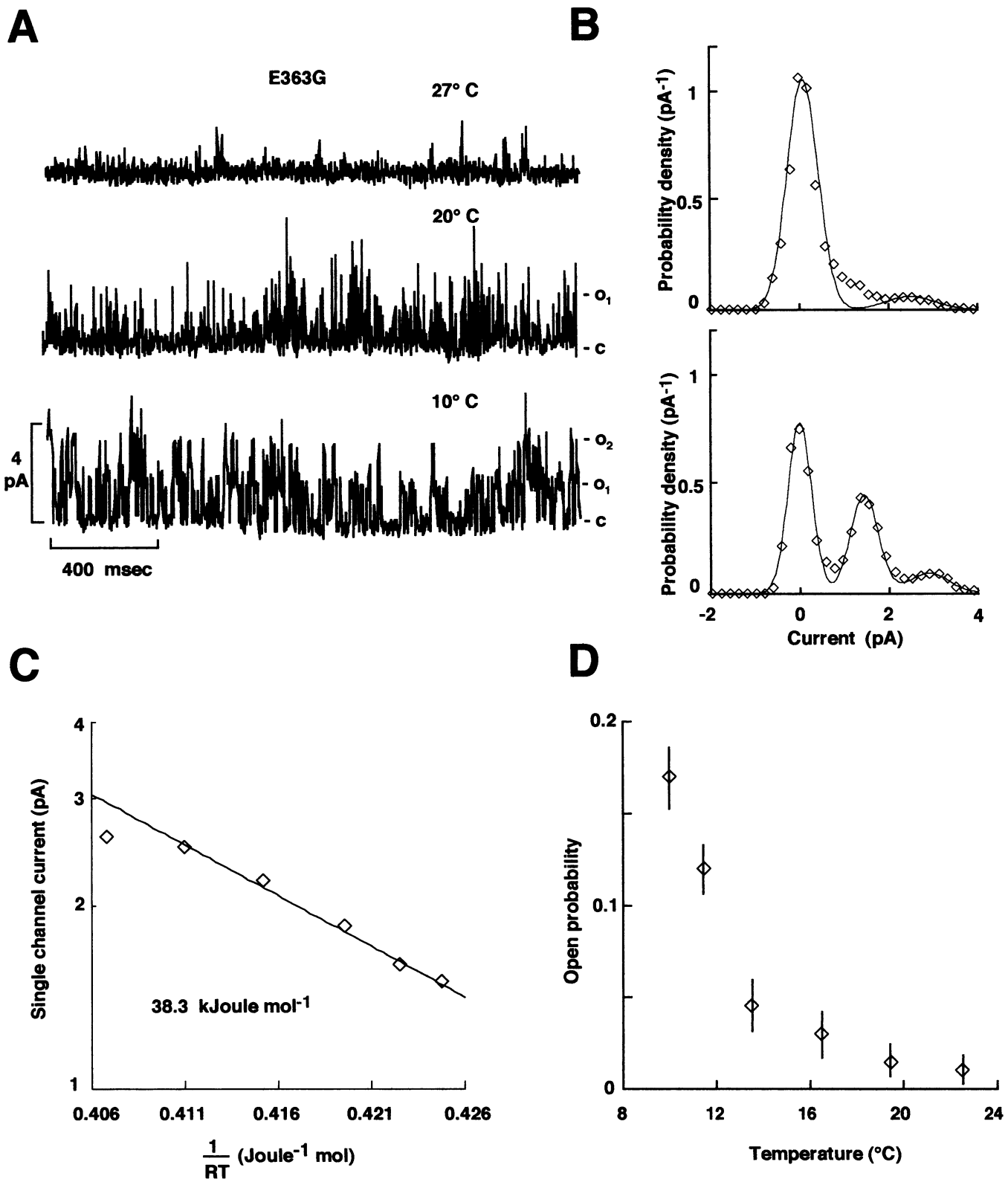

FIGURE 8 Dependence of single-channel properties of the mutant channel E363G on temperature. (*A*) Single-channel current recordings in the presence of a symmetrical solution containing 500 mM NaCl on both sides of the membrane in the presence of 500 μM cGMP at three different temperatures. Holding voltage was +60 mV. Data were filtered at 2 kHz. (*B*) Amplitude histograms at 19.5° and 10°C. (*C*) Dependence of the single-channel current at +60 mV on temperature in the presence of 500 mM NaCl on both sides of the membrane. The continuous line through the points yields an activation energy of 38.3 kJ mol^{-1}. (*D*) The dependence of the open probability on temperature. Data are from three patches.

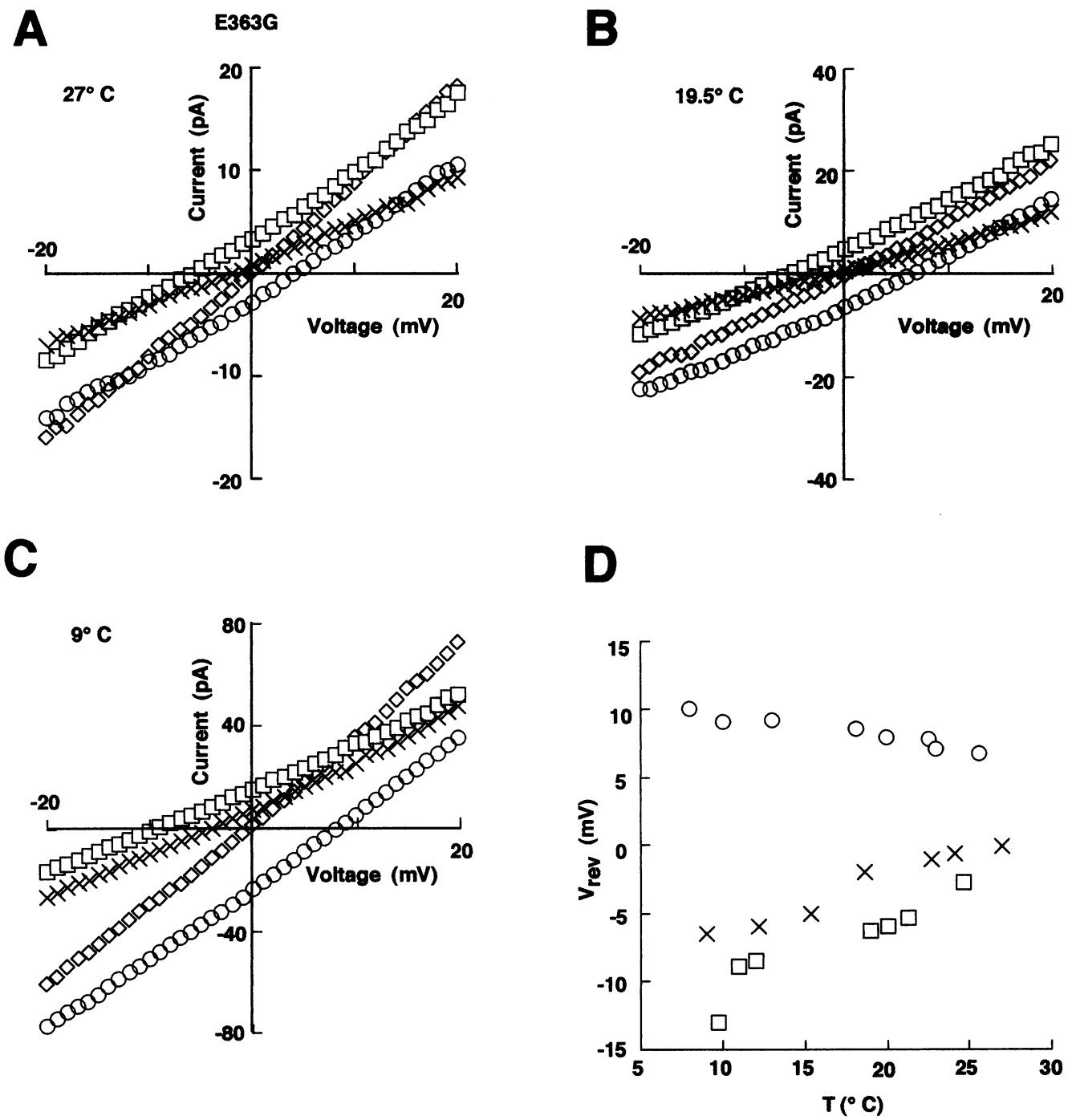

FIGURE 9 The effect of temperature on the reversal potential of the mutant channel E363G in biionic solutions. (*A, B,* and *C*) *I-V* relations in the presence of 500 μM cGMP and 110 mM Na^+ in the patch pipette and equimolar amounts of Na^+ ($\diamond$), Li^+ (○), Rb^+ (□), and Cs^+ (X) in the bathing medium at 27°, 19.5°, and 10°C, respectively. (*D*) Dependence of the reversal potential on temperature in the presence of 110 mM Na^+ in the patch pipette and equimolar amounts of Li^+ (○), Rb^+ (□), and Cs^+ (X) in the bathing medium.

the mutant channel E363G significantly depends on temperature.

DISCUSSION

A central problem in the understanding of the ionic permeation is the determination of physical and molecular factors causing ionic selectivity. In the presence of a thermodynamic equilibrium the Gibbs free energy can be introduced and assumed to regulate the ionic permeation. The Gibbs free energy is composed of an enthalpic term H and an entropic term $-TS$, and it may be expected that at room temperature (about 293° K) entropy cannot be neglected. However, from an experimental point of view,

it is not trivial to quantify the relative contribution of these two terms to the Gibbs free energy. To do so for the cGMP-activated channel, we have analyzed the effect of changing the temperature on the macroscopic current activated by 100 or 500 μM cyclic GMP and on the reversal potential between biionic solutions in the native and in the α subunit of the cGMP-activated channel. To relate the results of these experiments to estimates of the enthalpic and entropic contributions, a quantitative model of ionic permeation is necessary. Neither the native nor the α subunit of the cGMP channel can be described by a simple single-site model, and several features of the ionic permeation of Li^+ through both channels indicate a behavior of a multiion channel (Sesti et al., 1995). However, when the ionic activity of the permeating ions is reduced, both channels can be assumed to behave as a single ion channel (see Appendix). Under these conditions electrical measurements can be related to thermodynamic properties, as in the case of the K^+ channel of the sarcoplasmic reticulum (Miller et al., 1988).

Macroscopic versus single-channel current

As most of our analysis is based on the effect of temperature on macroscopic currents, it is important to evaluate the effect of temperature on the single-channel current and the open probability. In the native channel the macroscopic current carried by Na^+ was halved when the temperature was decreased by about 15°C (see Fig. 1). Sesti et al. (1994) have recently reported that the estimated single-channel conductance of the native channel was halved when the temperature was decreased by 16°C. In these experiments no evident effect of temperature on the open probability was observed, and the agreement between these two measurements suggests that varying the temperature between 15° and 25°C does not significantly change the open probability. Moreover, varying the temperature from 15° to 25°C does not change the open probability of the w.t. channel (see Fig. 6 *C*). The activation energies of a single-channel current and of the macroscopic current carried by NH_4^+ and Na^+ through the w.t. have very similar values (see Figs. 5 *A* and 6 *C*). These observations indicate that the activation energy of the macroscopic current can be assumed to be an estimate for the activation energy of a single open channel.

Activation energy in the native and in the α subunit

Table 1 summarizes the measurements of the activation energy of the current flowing at +100 mV (A+) and −100 mV (A−) in the native and w.t. channels. No significant dependence of the activation energy on the ionic activity was observed. At +100 mV (and −100 mV) in the native channel, the sequence of the activation energy for the various ions was

$$A_{NH_4^+} < A_{Na^+} \sim A_{K^+} < A_{Rb^+} < A_{Li^+} < A_{Cs^+}. \quad (3)$$

This sequence is different from the selectivity sequence, based on the reversal potential (see the values of v_{rev} reported in Table 2). At +100 mV the sequence of the activation energy in the w.t. channel was

$$A_{K^+} \sim A_{Na^+} \sim A_{NH_4^+} < A_{Li^+} < A_{Rb^+} < A_{Cs^+}, \quad (4)$$

and at −100 mV

$$A_{NH_4^+} < A_{Na^+} \sim A_{K^+} < A_{Rb^+} \sim A_{Li^+} < A_{Cs^+}. \quad (5)$$

The activation energy A of an ion is the energy barrier the ion has to cross to permeate through the channel. This energy is usually assumed to be the work necessary to move the ion from the bulk solution into the channel, i.e.,

$$A = E_h - E_c, \quad (6)$$

where E_h is the potential energy of the ion in the bulk solution (i.e., the hydration energy) and E_c is the energy of the interaction between the ion and the channel (Eisenman, 1962; Eisenman and Horn, 1983; Hille, 1992).

The hydration energy of alkali monovalent cations is known with a good accuracy to be 515, 405, 321, 296, and 263 kJ mol^{-1} for Li^+, Na^+, K^+, Rb^+, and Cs^+, respectively (Burgess, 1988) and is reported in Fig. 10, *A* and *B* (as crosses). These hydration energies can be described by the Born equation:

$$E_h = \frac{q^2}{8\pi\epsilon r}, \quad (7)$$

where q is the ion charge, r is the ionic radius, and ϵ is the water dielectric constant. Equation 7 provides ratios of hydration energies in agreement with those experimentally measured if the ionic radius of the alkali monovalent cations is assumed to be 0.78, 1.0, 1.26, 1.37, and 1.56 Å for Li^+, Na^+, K^+, Rb^+, and Cs^+, respectively. These values are slightly different from those usually reported for the same ions, i.e., 0.6, 0.95, 1.33, 1.48, and 1.69 Å (Burgess, 1988). Correct values of the hydration energies of monovalent alkali cations are obtained from Eq. 7, assuming the value 15×10^{-12} J^{-1} C^2 m^{-1} for ϵ (see Fig. 10, *A* and *B, solid lines through crosses*).

The term E_c represents the average potential energy of the permeating ion at the activated state. This potential energy will be due to electrostatic interactions with charged groups and with dipoles, Lennard Jones potentials, and potentials due to different degrees of oscillations (see, for instance, Brooks et al., 1988). A quantitative and detailed evaluation

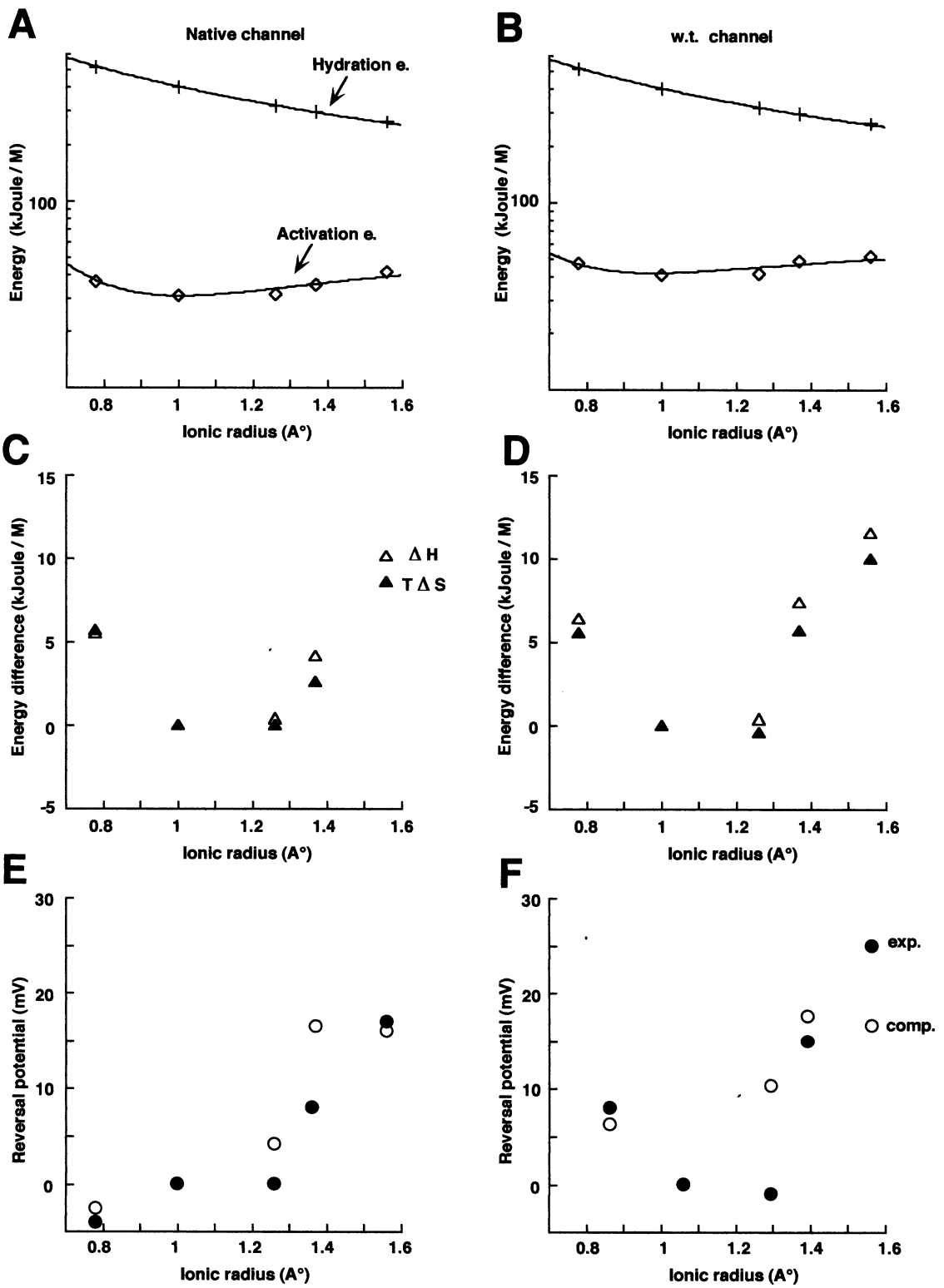

FIGURE 10 Activation energies and enthalpic and entropic contributions to ionic permeation in the native and w.t. channels. (*A* and *B*) Hydration (+) and activation (◇) energies for the native and w.t. channels, respectively. Hydration energies were obtained from Burgess (1988), activation energies were obtained from the data of Table 1 as the average between the activation energy at −100 and + 100 mV. The solid line through + was obtained from Eq. 6 and with the value of 15×10^{-12} J^{-1} C^2 m^{-1} for ϵ_0. The solid lines through ◇ were obtained from Eq. 8 and with the values of 1.28×10^3 kJ mol^{-1} Å^2 and 0.85 Å (*A*) and 1.15×10^3 kJ mol^{-1} Å^2 and 0.78 Å (*B*) for $q\mu_c/4\pi\epsilon$ and r_c, respectively. The ionic radius was assumed to be 0.76, 1, 1.26, 1.46, and 1.56 for Li^+, Na^+, K^+, Rb^+, and Cs^+, respectively (see text). (*C* and *D*) Enthalpic (△) and entropic (△) differences for the native and w.t. channels, respectively. Enthalpic differences ΔH were obtained from the data shown in *A* and *B* as the difference of the activation energy of ion X minus the activation energy of Na^+. Entropic differences $T\Delta S = T(S_x - S_{Na})$ at a temperature of 298°K were obtained from the data shown in Table 2 and Eq. A31. (*E* and *F*) Reversal potential of biionic solutions experimentally measured (●) and computed (○) from Eq. A11 for the native and w.t. channels, respectively.

of the term E_c is beyond the scope of this work and this simple expression will be used:

$$E_c = \frac{q\mu_c}{4\pi\epsilon(r + r_c)^2}. \quad (8)$$

Equation 8 describes the electrostatic interaction between the permeating ion and an electric dipole with momentum μ_c and length r_c. Thus the activation energies A for the different alkali cations are

$$A = \frac{q^2}{8\pi\epsilon r} - \frac{q\mu_c}{4\pi\epsilon(r + r_c)^2}. \quad (9)$$

Measured activation energies (Fig. 10, *diamonds*) can be accounted for by Eq. 9 using the values for $q\mu_c/4\pi\epsilon$ and r_c of 1.28 10^3 kJ mol^{-1}Å^2 and 0.85 Å for the native and the w.t. channels (Fig. 10 *A*) and 1.15 10^3 kJ mol^{-1} Å^2 and 0.78 Å for the w.t. channel (Fig. 10 *B*) as shown by the solid lines through the diamonds.

The good fit of the experimental activation energy with Eq. 9 suggests that the electrostatic energy of the permeating ion within the channel is dominated by ion-dipole interactions. This observation is in agreement with the presence of many amino acids (serine, threonine, etc.) with a significant electric dipole in the putative pore region of the α subunit (see Kaupp et al., 1989; Eismann et al., 1994).

The reversal potential in the native and in the α subunit

Table 2 summarizes the value of the reversal potential of biionic solutions in the presence of different ionic activities, in the native and w.t. channels. The values of v_{rev} were almost identical in the presence of 50 and 110 mM for the native channel. v_{rev} was slightly different when the ionic activity was reduced from 50 to 2.5 mM, especially for the w.t. channel. At a given ionic activity the values of reversal potentials of biionic solutions in the native and w.t. channels were similar but not identical. When 50 mM Li^+ was present in the patch pipette and an equimolar amount of Na^+ or K^+ was in the bathing medium, the reversal potential was about 4 mV in the native channel, and about −8 mV was in the α subunit. Therefore, the ionic selectivity, based on the reversal potential, is different in the two channels. When the reference ion, i.e., Li^+, was in the patch pipette and the tested ion was in the bathing medium, the reversal potential changed its sign, but its amplitude remained the same within the standard deviation.

Thermodynamic equilibrium

The ionic permeation through membrane channels is a thermally activated barrier crossing, which can be described by several approaches (Eyring et al., 1949; Lauger, 1982; Hanggi et al., 1990; Melnikov, 1991). It is evident that ionic permeation is a process with many degrees of freedom, and the existence of an entropic term is a consequence of the reduction of the degrees of freedom intrinsic to a macroscopic description. When thermodynamic equilibrium is present throughout the whole permeation process the usual thermodynamic quantities, such as the Gibbs free energy G, can be introduced, and enthalpic and entropic terms can be computed or estimated. Thermodynamic equilibrium is achieved in the presence of a rapid thermalization inside the wells or, more precisely, when the time of barrier crossing t_e is much longer than the time constant of fluctuations t_f inside the wells. Ions permeate through an ionic channel in about 10^{-7} s, and to have thermodynamic equilibrium ($t_f \ll t_e$), fluctuations inside the well must have frequencies not significantly lower than 1 GHz. This condition is likely to be satisfied when fluctuations inside the well are dominated by vibrations of bond length and angles, usually at frequencies in the THz range (Creighton, 1993; Brooks et al., 1988). Thermodynamic equilibrium cannot be assumed when the open channel is characterized by slower motions, such as those of large domains of the channel, with frequencies in the MHz range. In this case $t_f \approx t_e$, and there is no clear separation of time scales.

Estimation of enthalpic and entropic contribution to the Gibbs free energy

Given the values of the activation energies reported in Table 1 at +100 mV and −100 mV and assuming thermodynamic equilibrium, it is possible to derive an estimate of the enthalpic barrier for the various ions. As reported in the Appendix, the relation between A and the enthalpic barriers H_1 and H_2 can be rather complex; see Eqs. A24 and A25. To obtain a first approximation to the enthalpic barrier H, we will estimate this quantity as the average between the activation energy at +100 and −100 mV. From these estimates the enthalpic difference ΔH between ion X and Na^+ can be obtained:

$$\Delta H = H_x - H_{Na}, \quad (10)$$

and is plotted with open triangles in Fig. 10, *C* and *D*, for the native and w.t. channels, respectively. Similarly, it is possible to estimate the entropic difference between ion X and Na^+:

$$T\Delta S = T(S_x - S_{Na}), \quad (11)$$

from Eq. A31 and the values reported in Table 2. These quantities are plotted with filled triangles in Fig. 10, *C* and *D*, for the native and w.t. channels, respectively. The data reported in Fig. 10, *C* and *D*, clearly show that enthalpic and entropic differences have approximately the same value. This observation is not surprising in an ionic channel that is poorly selective and in which differences in the Gibbs free energy for the differentiations are small.

It is useful to verify whether the estimates of enthalpic and entropic differences reported in Fig. 10 are consistent with the experimental values of the reversal potential v_{rev}. The simple equation

$$Fv_{rev} = G_x - G_{Na} \quad (12)$$

can be used. The values of v_{rev} obtained from Eqs. 12 and A18 and the data of Fig. 10, *C* and *D*, are plotted with open circles in Fig. 10, *E* and *F*, and are compared with the experimentally determined values of v_{rev} (filled circles). The agreement between the computed and measured values of v_{rev} is satisfactory for the native channel (Fig. 10 *E*), whereas there are some discrepancies for K^+ and Cs^+ in the case of the w.t. channel (Fig. 10 *F*). However, the computed and experimentally determined values of v_{rev} agree within the standard deviation, which can be obtained from the data shown in Tables 1 and 2. The data reported in Fig. 10 and Tables 1 and 2 suggest some remarks. First, the greater selectivity of the native channel for Li^+ over Na^+ is caused primarily by a favorable entropic difference and not by a lower enthalpic barrier. Second, the enthalpic difference ΔH between Li^+ and Na^+ is larger in the w.t. than in the native channel, thus accounting for the difference in Li^+ versus Na^+ permeability between the native and the w.t. channels. Third, enthalpic differences between different cations are rather large but are compensated by opposing entropic effects. These observations indicate that entropic factors play a fundamental role in the determination of the ionic selectivity in the cGMP-gated channel from vertebrate rods. These conclusions are unaffected when the enthalpic barriers H_1 and H_2 are estimated by Eqs. A24 and A25 and entropic differences by Eqs. A29 and A30.

The ionic permeation in the w.t. channel and mutant channel E363G

The mutant channel E363G differs from the w.t. channel in that a neutral amino acid with the smallest residue is at position 363. To understand the role of the size of the narrowest section of the pore in the ionic permeation, it is instructive to compare the w.t. channel and mutant channel E363G. The mutant channel E363G is permeable to diethylammonium and triethylammonium, whereas the w.t. is not, suggesting that the w.t. channel and mutant channel E363G have an inner pore with an average radius of about 2.6 and 3.2 Å, respectively. The sequence of activation energy of the w.t. channel is significantly different from the sequence of hydration energy. In the mutant channel E363G, the sequence of activation energy is represented by sequence 2. The ionic conductivity in aqueous solution at 298°K is 38.7, 50.1, 73.5, 77.8, and 77.3 S cm^2 mol^{-1} for Li^+, Na^+, K^+, Rb^+, and Cs^+, respectively. It is evident that sequence 2 is almost the reverse of the conductivity sequence in aqueous solution, thus suggesting that alkali cations permeate through the mutant channel E363G almost in an hydrated form.

The dependence of v_{rev} on temperature is different in the w.t. channel and the mutant channel E363G. When Na^+ was inside the patch pipette and Cs^+ was in the bathing medium, dv_{rev}/dT was about -0.35 mV/°C in the w.t. (see Table 2) and 0.22 mV/°C in mutant channel E363G. A similar difference was also observed with Rb^+. The sequence of entropic contributions of the mutant channel E363G is consistent with the view that alkali cations permeate through the pore with a substantial water shell.

Microscopic interpretation of enthalpic and entropic terms

The enthalpic term of the barrier of the Gibbs free energy is essentially equal to the energy required to move the ion from the bulk solution into the channel at about its narrowest section. An alkali monovalent cation is usually surrounded by a number of water molecules, which can be on the order of 10 for Li^+ and about 4 for Cs^+; their hydrated radius is about 2.5 Å for Li^+ and about 3.5 Å for Cs^+ (Burgess, 1988). As the radius of the cGMP-gated channel is only slightly larger than 2 Å (Picco and Menini, 1993), monovalent alkali cations must reduce their hydration shell and loose some water molecules to permeate. The ion will lose these water molecules during its permeation through the channel vestibule and pore, and this process is expected to occur at several binding sites, where one water molecule is lost. Therefore, a realistic microscopic description of ionic permeation is one in which there are several binding sites, at which water molecules are exchanged. As a consequence, the profile of the Gibbs free energy has several barriers and peaks, and the value of the enthalpic contribution to the barrier of Gibbs free energy obtained here is essentially meant to be just an estimate of its order of magnitude.

The microscopic interpretation of the entropic term is less intuitive, and two factors have to be taken into account. First, when introduced in a partially ordered structure, such as water or a protein, large ions like Cs^+ will tend to create more disorder than a small ion like Li^+. The molar entropies of hydration are +11, +59, +101, +120, and +133 J K^{-1} mol^{-1} for Li^+, Na^+, K^+, Rb^+, and Cs^+, respectively (relative to zero for the proton). As a consequence, the tendency of large ions to create more disorder contributes to an entropic factor favoring the permeation of large ions such as Cs^+. Second, during the permeation through a restricted region, small ions will be able to cross in more configurations than larger ions. This second entropic factor has an opposite effect and will favor the ionic permeation of small ions such as Li^+. Given the relatively narrow size of the native and w.t. channels, ions are expected to permeate in a partially dehydrated state, and therefore the two entropic factors previously mentioned are likely to be relevant. As shown in Table 2 and Fig. 10, the sequence of entropic terms obtained from Eq. 11 is not a monotonic function of ionic radius. In this case Li^+ has a more favorable entropic

term than Na^+, presumably because it can cross the narrowest section of the pore in more configurations. Cs^+, however, has a more favorable entropic term than Na^+, presumably because it creates more disorder.

When ions can permeate through the channel without losing much of their water shell, the first factor will not contribute significantly to ionic selectivity. Indeed, in this case the hydration entropy of each ion in the bulk solution and in the channel will be the same. In contrast, the second factor may become relevant. In the case of mutant channel E363G, which has a significantly larger pore, with a radius of about 3.2 Å, the entropic term favors small ions, such as Li^+, and not large ones, such as Rb^+ or Cs^+.

It may be useful to conclude this thermodynamic analysis of ionic permeation with a final remark. An ion channel has a narrowest region, which can be measured and identified, and which in the w.t. cyclic GMP-activated channel is located near glutamate 363 (Bucossi et al., 1996). The narrowest region of an ionic channel may be part of the selectivity filter but does not necessarily constitute it; indeed, when glutamate 363 is neutralized to a glutamine, the ionic selectivity is hardly affected (see Table 3), whereas many other features of ionic permeation are (Root and MacKinnon, 1993; Eismann et al., 1994; Sesti et al., 1995; Park and MacKinnon, 1995). The present analysis of ionic selectivity in cyclic GMP-activated channels suggests that the molecular mechanisms underlying ionic selectivity are not restricted to one or very few amino acids and are more likely to be a global property of an ionic channel.

APPENDIX

This appendix is devoted to the estimation of enthalpic and entropic contributions from electrophysiological measurements. This estimation is simple for ionic channels that can be modeled as a one-ion pore, with equal electrical distances for all permeating ions and in which the offset peak condition is satisfied, such as in the K^+ channel from the sarcoplasmic reticulum (Miller et al., 1988). In this case, simple equations relate electrophysiological measurements to thermodynamic quantities. The cyclic GMP-gated channel is not a simple one-ion pore (Sesti et al., 1995), and therefore more complicated models must be analyzed.

The electrophysiological measurements to be related to enthalpy and entropy can be obtained from experiments involving a change in the temperature. In particular, it is possible to measure the activation energy A of the current I flowing at a given voltage and in the presence of a given ionic concentration, which is expected to depend on the temperature as

$$I = \text{const.}\ e^{-(A/RT)}, \tag{A1}$$

where const. is the usual preexponential factor. Equation A1 is expected to hold in the absence of any phase transition and when the temperature does not affect the gating of the channel. The activation energy A can be related to the enthalpic contribution H of the barrier height. In the presence of biionic solutions with ions X and Y at the outside and inside of the membrane, it is possible to measure the reversal potential v_{rev} as a function of temperature, i.e., dv_{rev}/dT, which can be related to the entropic difference $(S_x - S_y)$ between ions X and Y at the barrier peak. The exact relation between A and H and between dv_{rev}/dT and $(S_x - S_y)$ depends on the model used to describe the ionic permeation through the channel. We will consider the case of a one-ion channel with one or multiple binding sites and the case of a two-ion channel. It will be shown that in the low activity range (i.e., when the channel occupancy is low) all of these models can be approximated by the same kind of equations.

One binding site

This section recalls well-known properties of the ionic permeation through a pore with a single binding site (Hille, 1992). In this case the ionic permeation can be described by a Gibbs free energy profile with two barriers and one well that can be occupied by at most one single ion at any time (see Fig. 11 *A*). v is the voltage difference between the outside and inside of the membrane; the parameters of the model are the equivalent electrical distances d_o, d_2, d_3, and d_i; the barriers G_1 and G_2; and the well depth W. d_o is the electrical distance between the extracellular medium and the peak of barrier G_1, and d_i is the electrical distance between the intracellular medium and the peak of barrier G_2. These electrical distances satisfy the relation $d_o + d_2 + d_3 + d_i = 1$. Electrical distances, barrier heights, and well depth may be different for the various ions; d_{io}, d_{i2}, d_{i3}, and d_{ii} are the equivalent electrical distances; and G_{i1}, G_{i2}, and W_i are the barriers and well depth for the ionic species i. The ionic permeation is related to the above quantities through the transition rates k_{i1}, k_{i-1}, k_{i2}, and k_{i-2}.

In the case of monovalent cations, the transition rates k_{i1}, k_{i-1}, k_{i2}, and k_{i-2} for the ionic species i in the extracellular medium are related to the different parameters of the model as

$$k_{i1} = \nu e^{(G_{i1}/RT) - d_{io}V} \qquad k_{i-1} = \nu e^{(-(G_{i1}+W_i)/RT) + d_{i2}V}$$
$$k_{i2} = \nu e^{(-(G_{i2}+W_i)/RT) - d_{i3}V} \qquad k_{i-2} = \nu e^{(G_{i2}/RT) + d_{ii}V}, \tag{A2}$$

and, similarly, for the ionic species j in the intracellular medium, the transition rates h_{j1}, h_{j-1}, h_{j2}, and h_{j-2} are

$$h_{j1} = \nu e^{(-G_{j1}/RT) - d_{jo}V} \qquad h_{j-1} = \nu e^{(-(G_{j1}+W_j)/RT) + d_{j2}V}$$
$$h_{j2} = \nu e^{(-(G_{j2}+W_j)/RT) - d_{j3}V} \qquad h_{j-2} = \nu e^{(-G_{j2}/RT) + d_{ji}V}, \tag{A3}$$

where $V = Fv/RT$, F is the Faraday constant, $\nu = kT/h$, k is the Boltzman constant, and h is Planck's constant. The current I flowing in the presence of n different ionic species on the extracellular side and m different ionic species on the intracellular side is well known to be (Hille, 1992)

$$I = \frac{\sum_i^n (I_i[X_i]/K_i) - \sum_j^m (I_j[Y_j]/H_j)}{1 + \sum_i^n([X_i]/K_i) + \sum_j^m([Y_j]/H_j)}, \tag{A4}$$

where

$$I_i = -Fk_{i-1} \qquad I_j = -Fh_{j2}$$
$$K_i = \frac{k_{i-1} + k_{i2}}{k_{i-2}} \qquad H_j = \frac{h_{j-1} + h_{j2}}{h_{j1}}$$

$[X_i]$ is the activity of the ionic species X_i in the extracellular medium and $[Y_j]$ is the activity of the ionic species Y_j in the intracellular medium. In the presence of an identical concentration [X] of the same monovalent ionic species X on both sides of the membrane, Eq. A4 simplifies to

$$I = -F\frac{[X]}{1 + [X]^{\frac{k_1 + k_{-2}}{k_2 + k_{-1}}}}\left(\frac{k_{-1}k_{-2} - k_1k_2}{k_{-1} + k_2}\right), \tag{A5}$$

and in the low concentration limit, that is, when

$$I \approx -F[X]\frac{k_{-1}k_{-2} - k_1k_2}{k_{-1} + k_2}. \tag{A6}$$

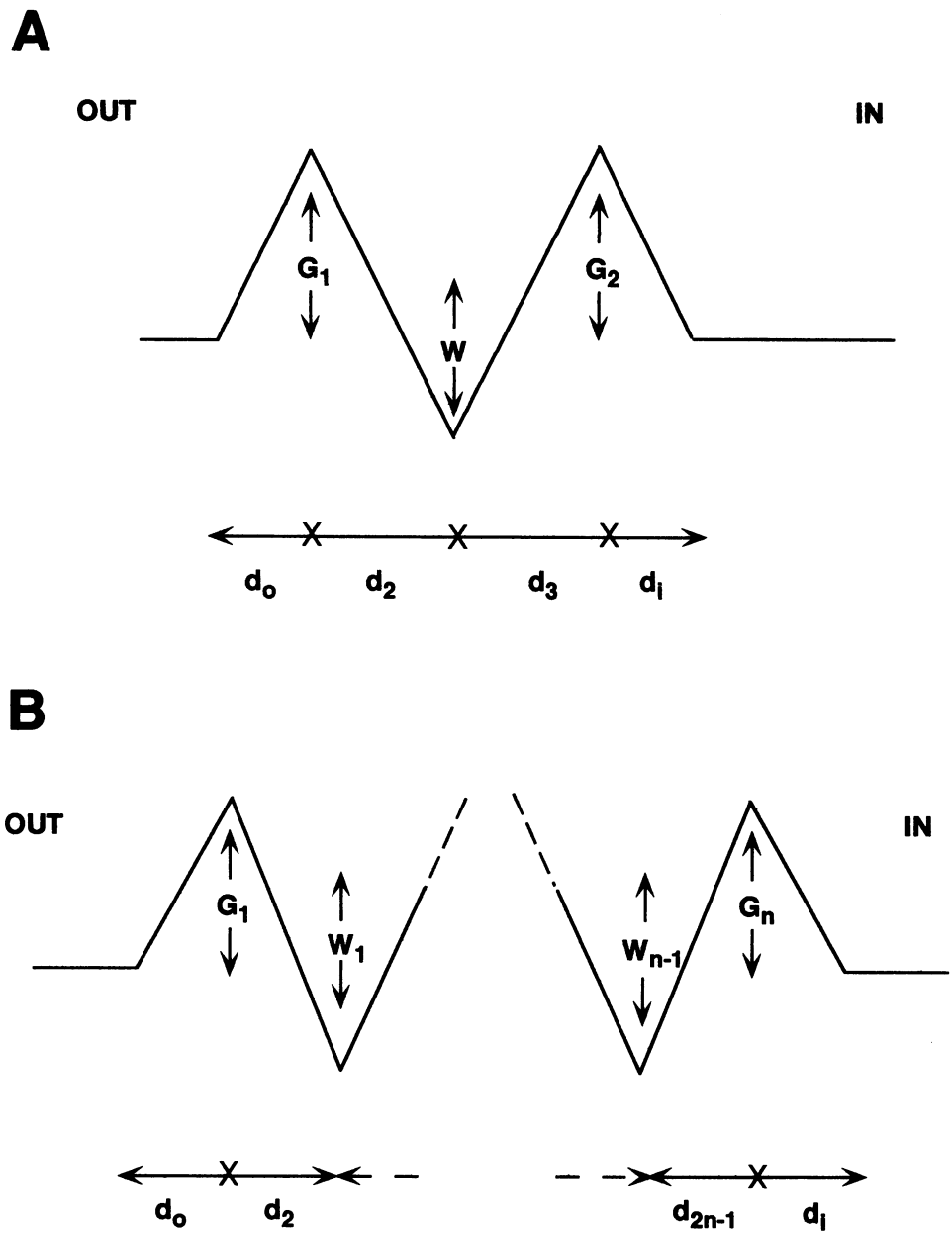

FIGURE 11 The Gibbs energy profile of a single ion channel with one binding site (*A*) and with n binding sites (*B*). Symbols are defined in the text.

Therefore, when $V \to \infty$ (i.e., when k_1 and k_2 become much smaller than k_{-1} and k_{-2}), we have $I \approx -F[X]k_{-2}$ or

$$I \approx -FT\,[X]e^{(-G_2/RT)+d_iV}. \tag{A7}$$

And when $V \to -\infty$ (i.e., when k_{-1} and k_{-2} become much smaller than k_1 and k_2), we have $I \approx F[X]k_1$, or

$$I \approx FT\,[X]e^{(-G_1/RT)-d_oV}. \tag{A8}$$

In the presence of the same concentrations of the ionic species X in the extracellular medium and of the ionic species Y in the intracellular medium, from Eq. A4 the current I is equal to zero at the reversal potential when

$$\frac{k_{-1}k_{-2}}{k_2 + k_{-1}} = \frac{h_1h_2}{h_2 + h_{-1}}. \tag{A9}$$

If electrical distances for the ionic species X and Y are the same, from Eqs. A2, A4, and A9 the $V_{rev} = Fv_{rev}/RT$ satisfies the equation

$$V_{rev} = \frac{G_{2x} - G_{2y}}{RT} + \ln[1 + e^{-(((G_{2x}-G_{1x})/RT)-(\delta_2+\delta_3)V_{rev}}] - \ln[1 + e^{-(((G_{2y}-G_{1y})/RT)-(\delta_2+\delta_3)V_{rev}}]. \tag{A10}$$

In the case of the offset peak conditions (i.e., when $G_{2x} - G_{1x} = G_{2y} - G_{1y} = G_x - G_y$), Eq. A10 simplifies to

$$Fv_{rev} = G_x - G_y. \tag{A11}$$

One ion pore with multiple binding sites

A channel with $n-1$ binding sites can be modeled by n consecutive barriers with height $G_1, G_2, \ldots G_n$, with G_1 and G_n facing the extracellular and intracellular media, respectively, by $n-1$ consecutive wells with depth $W_1, W_2, \ldots W_n - 1$ and by $2n$ electrical distances $d_o, d_2, \ldots d_{2n} - 1, d_i$, where d_o is the electrical distance between the extracellular medium and the peak of the barrier G_1, and d_i is the electrical distance between the peak of the barrier G_n and the intracellular medium. In this case and in the presence of the ionic species X in the extracellular medium and the ionic species Y in the intracellular medium, the current I flowing through a single channel depends on the activities of the ionic species X and Y asa

$$I = \frac{I_x([X]/K) - I_y([Y]/H)}{1 + ([X]/K) + ([Y]/H)}, \tag{A12}$$

where I_x and I_y are the maximum currents carried by the ionic species X and Y, respectively, and K and H denote the affinity of the channel for the ionic species X and Y, respectively. Equation A12 is obtained by some simple but tedious algebra from the kinetics scheme associated with the crossing of energy profile of Fig. 11 *B*. In the presence of an identical concentration of the same ionic species X on both sides of the membrane and in the low concentration limit, we obtain for $V \to +\infty$

$$I \approx -FT\,[X]e^{-(Gn/RT)+d_iV}, \tag{A13}$$

and for $V \to -\infty$,

$$I \approx -FT\,[X]e^{-(Gn/RT)-d_oV}, \tag{A14}$$

where k_1 is the transition rate from the extracellular medium across the barrier G_1, and $k - n$ is the transition rate from the intracellular medium across the barrier G_n.

Two ions pore with one binding site

There is evidence that the cyclic GMP-gated channel is a multiion channel with a major binding site. As a consequence, it is useful to also consider a scheme with a single binding site that can be occupied by two ions at the same time. In this scheme when one ion occupies the binding site, the ion will change the Gibbs energy profile experienced by other ions. The equations for such a scheme are

$$\begin{aligned}
&X_0 + C_x \underset{k_{-1}}{\overset{k_1}{\rightleftarrows}} C_x \xrightarrow{k_2} C_f + X_i \\
&X_0 + C_x \underset{h_{-1}}{\overset{h_1}{\rightleftarrows}} C_{2x} \xrightarrow{h_2} C_x + X_i \\
&Y_0 + C_f \xleftarrow[n_{-1}]{} C_y \underset{n_{-2}}{\overset{n_2}{\rightleftarrows}} C_f + Y_i \\
&Y_0 + C_y \xleftarrow[m_{-1}]{} C_{2y} \underset{m_{-2}}{\overset{m_2}{\rightleftarrows}} C_y + Y_i \\
&X_0 + C_y \underset{z_{-1}}{\overset{z_1}{\rightleftarrows}} C_{xy} \underset{z_{-2}}{\overset{z_2}{\rightleftarrows}} C_x + Y_i,
\end{aligned} \tag{A15}$$

where X_0 and Y_0 (X_i and Y_i) are the ionic species at the extracellular (intracellular) side of the channel. C_f, C_x, C_y, C_{2x}, C_{2y}, and C_{xy} indicate the channel with no ion inside, with one ion X, with one ion Y, with two ions X, with two ions Y, and with a pair of ions X and Y, respectively. The ionic species X(Y) is supposed to be present only at the extracellular (intracellular) side, and the ionic species Y_0 and X_i are quickly removed. From the scheme A15 at the steady state, the current I is

$$I = -F(C_y n_{-1} + C_{2y} m_{-1} - C_x k_2 - C_{2x} h_2), \tag{A16}$$

where

$$C_{2x} = C_1(x)C_x \qquad C_1(x) = \frac{h_1[X]}{h_2 + h_{-1}}$$

$$C_{2y} = C_2(y)C_y \qquad C_2(y) = \frac{m_{-2}[Y]}{m_2 + m_{-1}}$$

$$C_3(y) = \frac{z_{-2}[Y]}{z_2 + z_{-1}} \qquad C_4(x) = \frac{z_1[X]}{z_2 + z_{-1}}$$

$$C_y = \frac{n_{-2}[Y]A - k_1[X]C}{AD - BC} \qquad C_x = \frac{k_1[X]D - n_{-2}[Y]B}{AD - BC},$$

and $x = [X]$ and $y = [Y]$. The expressions for A, B, C, and D are

$$A = k_1[X](1 + C_1(x) + C_3(y)) + k_2 + k_{-1} + z_{-2}[Y] - z_2C_3(y)$$

$$B = k_1[X](1 + C_2(y) + C_4(x)) - z_2C_4(x)$$

$$C = n_{-2}[Y](1 + C_1(x) + C_3(y)) - z_{-1}C_3(y)$$

$$D = n_{-2}[Y](1 + C_2(y) + C_4(x)) + n_2 + n_{-1} - z_{-1}[X] + z_1C_4(x).$$

It is easy to see that in the low concentration range (i.e., when [X] and [Y] $\to 0$), $A \to k_2 + k - 1$ and $D \to n_2 + n - 1$, so that we have

$$I \approx -F\left(\frac{n_{-1}n_{-2}[Y]}{n_2 + n_{-1}} - \frac{k_1k_2[X]}{k_2 + k_{-1}}\right). \tag{A17}$$

It is evident that in the low activity range Eqs. A4, A12, and A17 have the same structure, indicating that in the low concentration range a two-ion pore with a single binding site behaves as a simple one-ion pore.

Estimation of the enthalpic barrier

The current flowing through an open channel is expected to depend on the absolute temperature T according to an Arrhenius relation (Atkins, 1978) as in Eq. A1. The activation energy A is related in a simple way to the enthalpic term H of the Gibbs free energy. The Gibbs free energy G is equal to

$$G = H - TS, \tag{A18}$$

where S is entropy. Therefore, at the two barriers 1 and 2 we have $G_1 = H_1 - TS_1$ and $G_2 = H_2 - TS_2$, where the new symbols have the obvious meaning. Equations A7 and A8 can be rewritten as

$$I \approx -FT\,[X]e^{S_2/R}e^{-(H_2/RT)+d_iV} \tag{A19}$$

$$I \approx FT\,[X]e^{S_1/R}e^{-(H_1/RT)-d_oV}. \tag{A20}$$

By differentiating Eqs. A19 and A20 with respect to T we obtain

$$\frac{H_2}{RT} = \frac{dI}{dT}\cdot\frac{T}{I} - 1 + d_iV, \tag{A21}$$

and

$$\frac{H_1}{RT} = \frac{dI}{dT}\cdot\frac{T}{I} - 1 - d_o V. \quad \text{(A22)}$$

From Eq. A1 we have

$$\frac{dI}{dT}\frac{T}{I} = \frac{A}{RT}. \quad \text{(A23)}$$

Therefore, an estimate of the enthalpic term for H_2 is

$$A_+ + (-1 + d_i V)RT, \quad \text{(A24)}$$

and for H_1 is

$$A_- + (-1 - d_o V)RT, \quad \text{(A25)}$$

where A_- and A_+ are the activation energies at very negative and very positive membrane potentials.

Estimation of the electrical distances

To obtain an estimate of the enthalpic barrier from the activation energy, it is necessary to have a value for the equivalent electrical distances d_o and d_i. In the native channel the shape of the *I-V* relations in the presence of symmetrical solutions depended on the nature of the permeating ion, suggesting that the electrical distances were different for the various ions. These quantities were estimated as described for Li^+ and Na^+ by Sesti et al. (1995). For the native channel the equivalent electrical distance d_o was assumed to be 0.1 for Li^+, Na^+, K^+, Rb^+, Cs^+, and NH_4^+, and d_i to be 0.18, 0.14, 0.2, 0.3, 0.35, and 0.04 for the same ionic species, respectively. For the w.t. channel the shape of the *I-V* relations in the presence of symmetrical solutions containing alkali monovalent cations or NH_4^+ was the same. As a consequence, d_o and d_i were assumed to have the same value, 0.25, for all tested cations.

Estimation of the entropy difference between two ions

Consider two ionic species X and Y at the extracellular and intracellular sides of the membrane, with equivalent electrical distances d_o, d_2, d_3, and d_i and δ_o, δ_2, δ_3, and δ_i with barrier heights G_{1x}, G_{2x} and G_{1y}, G_{2y} and well depth W_x and W_y for X and Y, respectively. At the reversal potential, Eq. A9 is satisfied and we obtain

$$e^{\alpha V_{rev}} = \frac{e^{-(G_{1y}+G_{2y}/RT)}e^{-(G_{1x}/RT)+d_2V_{rev}} + e^{-(G_{2x}/RT)-d_3V_{rev}}}{e^{-(G_{1x}+G_{2x}/RT)}e^{-(G_{2y}/RT)-\delta_3V_{rev}} + e^{-(G_{1y}/RT)+\delta_2V_{rev}}}, \quad \text{(A26)}$$

where $\alpha = d_2 + d_i + \delta_o + \delta_3$. By rearranging Eq. A26 and differentiating with respect to T, it is possible to derive an equation for the entropy difference at barrier 1 between the two ions:

$$S_{1x} - S_{1y} = -\frac{d}{dT}(G_{1x} - G_{1y}) = -\alpha F\frac{dv_{rev}}{dT} - \frac{d}{dT}Z_1(V_{rev}), \quad \text{(A27)}$$

where

$$Z_1(V_{rev}) = RT\ln\frac{e^{-d_3V_{rev}} + e^{-(G_{1x}-G_{2x}/RT)+d_2V_{rev}}}{e^{-\delta_3V_{rev}} + e^{-(G_{1y}-G_{2y}/RT)+\delta_2V_{rev}}},$$

and at barrier 2,

$$S_{2x} - S_{2y} - -\frac{d}{dT}(G_{2x} - G_{2y}) = -\alpha F\frac{dv_{rev}}{dT} - \frac{d}{dT}Z_2(V_{rev}), \quad \text{(A28)}$$

where

$$Z_2(V_{rev}) = RT\ln\frac{e^{d_2V_{rev}} + e^{-(G_{2x}-G_{1x}/RT)-d_3V_{rev}}}{e^{\delta_2V_{rev}} + e^{-(G_{2y}-G_{1y}/RT)-\delta_3V_{rev}}}.$$

When the shape of the *I-V* relations does not change with temperature the terms $d/dT[(G_{IX})/RT-(G_{2X})/RT]$ and $d/dT[(G_{IY})/RT-(G_{2Y}/RT]$ can be assumed to be negligible. Given the values of v_{rev} reported in Table 2, we can assume also that . Under these assumptions Eqs. A27 and A28 simplify to

$$S_{1x} - S_{1y} = -\frac{Fdv_{rev}}{dT} \times\left(\alpha + \frac{-d_3e^{-d_3V_{rev}+d_2}e^{-(G_{2x}-G_{1x}/RT)+d_2V_{rev}}}{e^{-d_3V_{rev}} + e^{-(G_{2x}-G_{1x}/RT)+d_2V_{rev}}} + \frac{-\delta_3e^{-\delta_3V_{rev}} + \delta_2e^{-(G_{2y}-G_{1y}/RT)+\delta_2V_{rev}}}{e^{-\delta_3V_{rev}} + e^{-(G_{2y}-G_{1y}/RT)+\delta_2V_{rev}}}\right) + \frac{Z_1(V_{rev})}{T}, \quad \text{(A29)}$$

and

$$S_{2x} - S_{2y} = -\frac{Fdv_{rev}}{dT} \times\left(\alpha + \frac{d_2e^{d_2V_{rev}} - d_3e^{-(G_{2x}-G_{1x}/RT)-d_3V_{rev}}}{e^{d_2V_{rev}} + e^{-(G_{2x}-G_{1x}/RT)-d_3V_{rev}}} + \frac{\delta_2e^{\delta_2V_{rev}} - \delta_3e^{-(G_{2x}-G_{1x}/RT)-\delta_3V_{rev}}}{e^{\delta_2V_{rev}} + e^{-(G_{2x}-G_{1x}/RT)-\delta_3V_{rev}}}\right) + \frac{Z_2(V_{rev})}{T}. \quad \text{(A30)}$$

If the electrical distances for the two ionic species are the same and in the simple case of the offset peak condition, $G_{1x} - G_{1y} = G_{2x} - G_{2y} = G_x - G_y$, we obtain the simple Eq. A11 and the entropy difference $S_x - S_y$ can be easily evaluated as

$$S_x - S_y - -F\frac{dv_{rev}}{dT}. \quad \text{(A31)}$$

Given the estimated values of electrical distances and barrier heights (see also Sesti et al., 1995), the values of entropy difference obtained with Eqs. A29 and A30 and from Eq. A31 for the native channel did not differ by more than 30%. As a consequence, the entropy difference was estimated with the simple Eq. A31.

We are grateful to Dr. Maria Teresa Giraudo, who collaborated with us on preliminary experiments. Prof. Benjamin U. Kaupp and Dr. Elisabeth Eismann kindly provided us with mRNA of the w.t. channel and mutant channels and gave us very useful suggestions. We are indebted to Dr. A.

Menini for her critical reading of the manuscript. The experimental part of this work was made possible by the help and advice of Dr. L. Spadavecchia, who built the Peltier device to control the temperature, and F. Conforti, G. Franzone, E. Vigo, and C. Pizzorno, who built the mechanical parts of the experimental set-up. We appreciate the help of Miss M. Zanini, who kindly typed the manuscript, and Miss L. Giovanelli, who did the artwork and checked the English.

This research was supported by grants funded by the European Community (SSS 6961, Human Capital and Mobility Programme) and by the Human Frontier Science Program.

REFERENCES

Atkins, P. W. 1978. Physical Chemistry. Oxford University Press, Oxford.

Brooks, C. A., III, M. Karplus, and B. M. Pettitt. 1988. Proteins: A Theoretical Perspective of Dynamics, Structure and Thermodynamics. John Wiley and Sons, New York.

Bucossi, G., E. Eismann, F. Sesti, M. Nizzari, M. Seri, U. B. Kaupp, and V. Torre. 1996. Time dependent current decline in cyclic GMP gated channels caused by point mutations in the pore region. *J. Physiol. (Lond.).* In press.

Burgess, J. 1988. Ions in Solution. Ellis Horwood Limited, Chichester.

Chen, T. Y., Y. W. Peng, R. S. Dhallan, B. Ahamed, R. R. Reed, and K. W. Yau. 1993. A new subunit of the cyclic nucleotide-gated cation channel in retinal rods. *Nature.* 362:764–767.

Creighton, T. E. 1993. Proteins: Structures and Molecular Properties. Freeman, New York. In press.

Eisenman, G. 1962. Cation selective glass electrodes and their mode of operation. *Biophys. J.* 2(Suppl. 2):259–323.

Eisenman, G., and R. Horn. 1983. Ionic selectivity revisited: the role of kinetic and equilibrium processes in ion permeation through channels. *J. Membr. Biol.* 76:197–225.

Eismann, E., F. Muller, S. Heinemann, and B. Kaupp. 1994. A single negative charge within the pore region of a cGMP-gated channel controls rectification, Ca^{2+} blockage, and ionic selectivity. *Proc. Natl. Acad. Sci. USA.* 91:1109–1113.

Eyring, H. R., R. Lumry, and J. W. Woodbury. 1949. Some application of modern rate theory to physiological systems. *Rec. Chem. Prog.* 10: 100–114.

Fesenko, E. E., S. S. Kolesnikov, and A. L. Lyubarsky. 1985. Induction by cyclic GMP of cationic conductance in plasma membrane of retinal rod outer segment. *Nature.* 313:310–313.

Furman, R. E., and J. C. Tanaka. 1990. Monovalent selectivity of the cyclic guanosine monophosphate-activated ion channel. *J. Gen. Physiol.* 96: 57–82.

Hamill, O. P., A. Marty, E. Neher, B. Sakmann, and F. J. Sigworth. 1981. Improved patch-clamp techniques for high resolution current recording from cells and cell-free membrane patches. *Pflugers Arch.* 391:85–100.

Hanggi, P., P. Talkner, and M. Borkovec. 1990. Reaction-rate theory: fifty years after Kramer. *Rev. Mod. Phys.* 62:251–341.

Hille, B. 1992. Ionic Channels of Excitable Membranes. Sinauer Associates, Sunderland, MA.

Kaupp, U. B., T. Niidome, T. Tanabe, S. Terada, W. Bonigk, W. Stuehmer, N. J. Cook, K. Kangawa, H. Matsuo, T. Hirose, T. Miyata, and S. Numa. 1989. Primary structure and functional expression from complementary DNA of the rod photoreceptor cyclic GMP-gated channel. *Nature.* 342:762–766.

Körschen, H., M. Illing, R. Seifert, F. Sesti, A. Williams, S. Gotzes, S. Colville, F. Miller, A. Dose, M. Godde, L. Molday, U. B. Kaupp, and R. S. Molday. 1995. A 240 K protein with a bipartite structure represents the complete β-subunit of the cyclic nucleotide-gated channel from rod photoreceptor. *Neuron.* 15:627–636.

Lauger, P. 1982. Microscopic calculation of ion-transport rates in membrane channels. *Biophys. Chem.* 15:89–100.

Luehring, H., W. Hanke, R. Simmoteit, and U. B. Kaupp. 1990. Cation selectivity of the cyclic GMP-gated channel of mammalian rod photoreceptors. *In* Sensory Transduction. A. Borsellino, L. Cervetto, and V. Torre, editors. Plenum Press, New York. 169–174.

Melnikov, V. I. 1991. The Kramers problem: fifty years of development. *Phys. Rep.* 209:1–71.

Menini, A. 1990. Currents carried by monovalent cations through cyclic GMP-activated channels in excised patches from salamander rods. *J. Physiol. (Lond.).* 424:167–185.

Miller, C., N. Stahl, and M. Barrol. 1988. A thermodynamic analysis of monovalent cation permeation through a K^+ selective ion channel. *Neuron.* 1:159–164.

Nizzari, M., F. Sesti, M. T. Giraudo, C. Virginio, A. Cattaneo, and V. Torre. 1993. Single channel properties of a cloned channel activated by cGMP. *Proc. R. Soc. Lond.* 254:69–74.

Park, C. S., and R. MacKinnon. 1995. Divalent cation selectivity of an ion binding site in the pore of a cyclic nucleotide-gated channel. *Biophys. J.* 68:A129.

Picco, C., and A. Menini. 1993. The permeability of the cGMP-activated channel to organic cations in retinal rods of the tiger salamander. *J. Physiol. (Lond.).* 460:741–758.

Root, M. J., and R. MacKinnon. 1993. Identification of an external divalent binding site in the pore of a cGMP-activated channel. *Neuron.* 11: 459–466.

Sesti, F., E. Eismann, B. U. Kaupp, M. Nizzari, and V. Torre. 1995. The multi-ion nature of the cGMP-gated channel from vertebrate rods. *J. Physiol. (Lond.).* 487–1:17–36.

Sesti, F., M. Straforini, T. D. Lamb, and V. Torre. 1994. Properties of single channels activated by cyclic GMP in retinal rods of the tiger salamander. *J. Physiol. (Lond.).* 474–2:203–222.

Taylor, W. R., and D. A. Baylor. 1995. Conductance and kinetics of single cGMP-activated channels in salamander rod outer segments. *J. Physiol. (Lond.).* 483:567–582.